Applied Physics
Express

The Japan Society
of Applied Physics

APEX REVIEW • OPEN ACCESS

Biochemical pathways for device nanoarchitectonics: organic semiconductors interfaced with biomolecular systems

To cite this article: Takuma Ohashi *et al* 2026 *Appl. Phys. Express* **19** 040106

Applied Physics Express **19**, 040106 (2026)

APEX REVIEW

https://doi.org/10.35848/1882-0786/ae6166

Biochemical pathways for device nanoarchitectonics: organic semiconductors interfaced with biomolecular systems

Takuma Ohashi[1,2], Linawati Sutrisno[3], Yu Yamashita[1,4], and Katsuhiko Ariga[1,2,4*]

[1]*Research Center for Materials Nanoarchitectonics (MANA), National Institute for Materials Science (NIMS), 1-1 Namiki, Tsukuba, Ibaraki 305-0044, Japan*
[2]*Graduate School of Science and Technology, Tokyo University of Science, 2641 Yamazaki, Noda, 278-8510, Japan*
[3]*International Center for Young Scientists (ICYS), National Institute for Materials Science, 1-1 Namiki, Tsukuba, Ibaraki 305-0044, Japan*
[4]*The Department of Advanced Materials Science, Graduate School of Frontier Sciences, The University of Tokyo, 5-1-5 Kashiwanoha, Kashiwa, Chiba 277-8561, Japan*

[*]E-mail: ARIGA.Katsuhiko@nims.go.jp

Received March 16, 2026; revised April 7, 2026; accepted April 17, 2026; published online April 30, 2026

This review discusses organic semiconductors interfaced with biomolecular systems, focusing on the construction of material systems through biochemical pathways for device nanoarchitectonics. The initial section highlights biosensors as representative applications at the interface of device engineering and biosystem science. The subsequent sections describe nanoarchitectonics approaches for the synthesis and organization of organic semiconductor devices using bioprocessing. In particular, doping of organic semiconductors in water under ambient conditions coupled with bioprocessing are emphasized, including proton-coupled electron transfer and sugar redox reactions. Inspired by the sophisticated molecular architectures that enables ultra-high-level functions in biological systems, nanoarchitectonics is expected to facilitate further advances in organic semiconductor biodevices.

1. Introduction

Human civilization depends on the availability of materials, machines, and devices, and advances in these technologies have significantly improved our quality of life. From a materials perspective, scientific progress during the 20th century represented a major turning point. In addition to naturally occurring substances, developments in various fields of chemistry have enabled the creation of a wide range of new materials. This trend continues today in chemistry-related disciplines such as organic chemistry,[1–4] inorganic chemistry,[5–8] polymer chemistry,[9–12] supramolecular chemistry,[13–16] coordination chemistry,[17–20] materials chemistry,[21–24] and biochemistry.[25–28] Physics also plays an essential role in the detailed investigation of the physical properties of these materials. In particular, the development of highly accurate, high-resolution analytical techniques has clarified the fundamental principles underlying the properties and mechanisms of microstructures and nanostructures.[29–31] Owing to these advances in chemistry and physics, it has become widely recognized that controlling nanostructures and their properties at the nanoscale is crucial.[32–34] The properties of a given material can vary dramatically depending on its nanostructures. In some cases, precise control of nanostructure can lead to unique properties and highly functional systems.[35–37] In this context, the emergence of the concept of nanotechnology marked a critical step in this scientific trend.[38,39]

Nanotechnology has enabled the observation[40–42] and manipulation[43,44] of structures at atomic and molecular levels. Furthermore, it has significantly advanced the characterization of physical properties at these corresponding scales.[45–48] These developments have deepened our understanding of the fundamental principles governing nanoscale physics. Such knowledge should now be applied to the development of functional materials. Nanoarchitectonics, a post-nanotechnology concept, has been proposed to achieve this goal (Fig. 1).[49] It involves constructing functional material systems from atomic- and molecular-scale building blocks.[50–52] By integrating nanotechnology with materials chemistry and physics, nanoarchitectonics provides a comprehensive framework for the creation of functional materials. In this approach, materials are assembled using a variety of techniques, including atomic and molecular manipulation, chemical transformations (including organic synthesis), physical transformations, self-assembly and self-organization, alignment and structurization induced by external forces or fields, micro- and nanofabrication, and biochemical processes.[53–55] This concept emphasizes the integration of multiple technologies, and the construction process often involves multiple stages. Compared with single-step self-assembly, nanoarchitectonics is particularly advantageous for fabricating asymmetric and hierarchical structures.[56] Because all materials are composed of atoms and molecules, nanoarchitectonics can, in principle, be applied to the creation of virtually any material system. If the ultimate theory of physics is regarded as a "theory of everything,"[57] nanoarchitectonics may be considered a methodology applicable to virtually everything in materials science.[58,59]

Although the term "nanoarchitectonics" is relatively new, the fundamental concepts underlying this methodology have been explored for decades. Two representative examples can be considered—one artificial and the other natural. The first example is the development of devices such as highly integrated circuits, which have progressed through increasing levels of integration enabled by ultrafine processing technologies. Subsequently, the importance of various material innovations,[60–63] quantum effects,[64–66] and structural organization techniques—such as interface manipulation,[67–69] and supramolecular organization[70–72] —has become evident. Device development is therefore a field in which the integration of top-down and bottom-up processes is steadily advancing. This research and technological field can be regarded as a

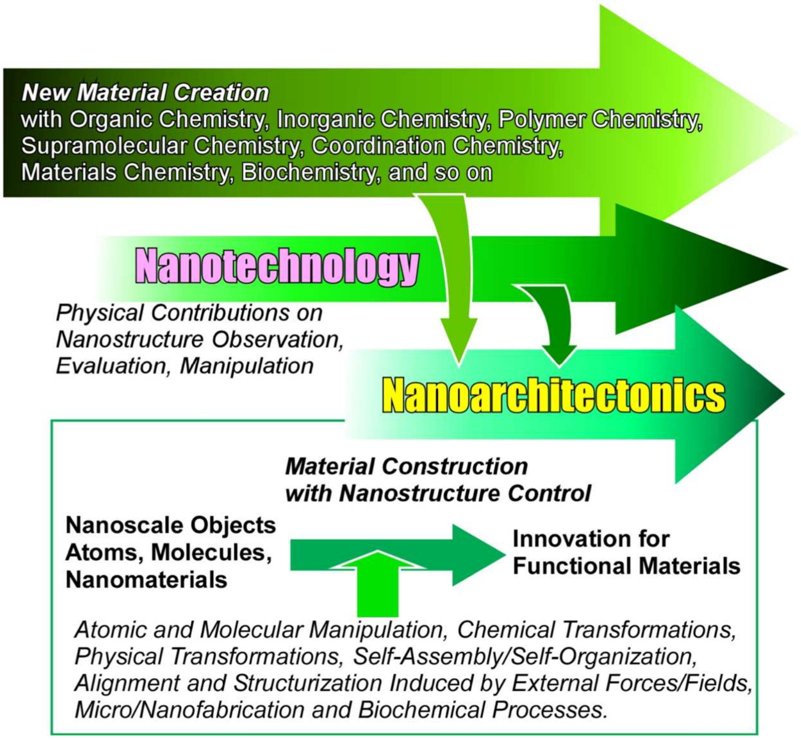

Fig. 1. Outline of nanoarchitectonics, a post-nanotechnology concept, for constructing functional material systems from atomic and molecular-scale objects through fusing nanotechnology with material chemistry and physics.

representative example of nanoarchitectonics as a comprehensive approach for constructing functional structures.73–75)

Biofunctional structures provides prime examples of successful molecular architectures, and demonstrate the potential for constructing functional material systems based on concepts similar to nanoarchitectonics. In various biological systems, including those involved in photosynthesis,76,77) functional molecules are arranged in a highly organized manner, enabling the execution of complex functions. These structures are as if functional molecules were assembled according to an ingenious blueprint. Such biological systems can therefore be regarded instructive models for nanoarchitectonics.77–79) Examples like these provide important inspiration for the development of nanoarchitectonics strategies. To construct such advanced functional systems, we should aim to achieve in a few decades what nature has accomplished over billions of years.

Integrating these two successful concepts of nanoarchitectonics—artificial device fabrication and biological functional systems—is highly significant. In particular, this integration leads to device development involving bioprocesses. This review discusses the development of device materials utilizing bioprocesses and devices from the perspective of nanoarchitectonics. Accordingly, we focus on materials that can function from intermediaries between biosystems and electronic devices. Such materials are soft and flexible, similar to biosystems, while possessing specific electronic functions. Representative candidates include conductive polymers80–82) and organic semiconductors83–85) including polymeric semiconductors.86–88) Consequently, this review primarily focus on the coupling of organic semiconductor nanoarchitectonics with bioprocesses for device applications.

With this background, we briefly summarize the advantages of organic semiconductors and explain why they have attracted considerable attention. Organic semiconductors are composed of organic compounds and exhibit several advantages compared with conventional inorganic semiconductors such as silicon. These advantages includes low cost, light weight, ease of fabrication, and compatibility with flexible substrates. In addition, organic semiconductors offer a significant advantage in terms of functionality because their properties can be readily tailored through molecular design.89–91) For example, substituents can be introduced and the length of aromatic conjugation can be adjusted to optimize performance for specific applications. Furthermore, organic semiconductors with systematically varied molecular structures can be synthesized. Low-temperature processing is also possible, and large-area thin films can be readily fabricated using solution-based processes.92–94) Thus, organic semiconductors are well suited to nanoarchitectonics involving molecular design and the fabrication of thin-film structures.

Accordingly, this review discusses "organic semiconductors interfaced with biomolecular systems," with a focus on the constructing material systems through "biochemical pathways for device nanoarchitectonics." Biological processes offer several advantages, including low environmental impact, high specificity and selectivity, and low toxicity to the human body. In addition, biomolecular reactions enable precise control of electron transfer, which can be utilized in the development of electronic materials. The flexibility and lightweight nature of organic semiconductors also make them promising candidates for wearable devices.95–97) Therefore, incorporating biomolecular processes that exert minimal impact on the human body is highly attractive for the development of such devices. This review highlights recent research trends in organic semiconductors systems that employ biomolecular processes.

The following section focuses on biosensors as representative examples of applications at the interface between device engineering and biosystem science. Several examples involving both small molecules and polymers are presented to illustrate the potential functionalities of organic semiconductors when interfaced with biomolecular systems. The subsequent section discusses nanoarchitectonics approaches for the synthesis and organization of organic semiconductor devices, with particular emphasis on bioprocessing. This includes the fabrication of electronic materials through bioprocesses and the organization of device materials within interfacial environments. The next section addresses nanoarchitectonics related to doping, which is essential for the processing of organic semiconductors. First, a general overview of doping is provided as a methodological guide, followed by recent examples of its coupling with bioprocessing, including proton-coupled electron transfer (PCET) and sugar redox reactions. In addition, examples of device stabilization through bioprocessing are introduced. Although the integration of bioprocessing with organic semiconductor engineering is a relatively recent development, it holds significant potential. The final section discusses future perspectives. This review aims to stimulate further exploration of biological reactions in the fields of organic semiconductors and nanomaterials research.

2. Usage examples of organic semiconductor device for biology: biosensor

First, we provide an overview of the relationship between bioprocesses and organic semiconductor devices using examples to illustrate this. Biosensors are devices that interface with biological systems. We then provide brief examples of biosensors that use organic semiconductors, and give an overview of their structures and target materials.

We focus on two types of transistor structures used for sensing: organic electrochemical transistors (OECTs) and extended-gate field-effect transistors. OECTs use electrolytes consisting of aqueous solutions or ionic liquids and offer greater capacitance and transconductance than solid-state thin-film transistors. Consequently, they can be driven by extremely low voltages. Conversely, extended-gate transistors are constructed by attaching an extended gate to an existing organic field-effect transistor (OFET), which enables the OFET to be operated in a dry environment. This avoids water, which contributes to device degradation, and enables long-term stable operation. Below, we introduce the specific sensing targets and analytical methods employed with these devices.

2.1. Biosensor for small molecular gest

2.1.1. Glucose sensor. Abnormal blood glucose levels and impaired regulation of glucose metabolism can cause serious health problems, making the development of affordable glucose sensors essential for effective health management on an individual level. OECTs have emerged as a promising platform for biosensing applications due to their inherent advantages, such as low operating voltage requirements and exceptional sensitivity. Glucose detection can be achieved by immobilizing the glucose-selective glucose oxidase on the gate electrode. Several examples employing p-type channels based on PEDOT:PSS have been reported. One representative case, reported by Berggren, Stavrinidou and co-workers [Fig. 2(a)], involves a gate electrode functionalized with platinum nanoparticles and glucose oxidase.98) In this system, the addition of glucose triggers an enzyme-catalyzed redox reaction that generates hydrogen peroxide. The Pt nanoparticles on the gate subsequently oxidize the hydrogen peroxide, leading to electron transfer and a shift in the effective gate potential, which results in a decrease in the channel current. Specifically, glucose export was directly monitored in isolated chloroplasts from tobacco plants. The OECT sensor was interfaced with the chloroplasts, enabling the detection of glucose release with a time resolution of 1 min.

In contrast, Xu and co-workers reported the use of an n-type conductive polymer, the polymeric semiconductor poly (benzimidazobenzophenanthroline) (BBL), as the channel material in an OECT [Fig. 2(b)].99) In this system, ferrocene was co-immobilized with glucose oxidase on the gate electrode, serving as an electron mediator to enhance the efficiency of electron transfer between the gold electrode and glucose oxidase. The BBL exhibited high performance and stability in aqueous electrolyte solutions. Stability tests confirmed consistent performance under multiple cycles and continuous stress, demonstrating the long-term stability and reliability of the sensor. Overall, the n-type polymer semiconductor-based OECT glucose sensor exhibited promising performance, stability and flexibility, highlighting its strong potential for practical glucose sensing applications.

2.1.2. Lactate sensor. Lactate is one of the key metabolic products in the anaerobic phase of glycolysis and an important biomarker in clinical diagnosis and sports medicine.100,101) Although blood lactate levels have traditionally been used for measurement, a positive correlation has been observed between blood and sweat lactate concentrations.102,103) This makes sweat lactate measurement a noninvasive method for quantitatively detecting lactate. Since lactate oxidase is selective for lactate, it can be detected by immobilizing it on the gate electrode or channel of an OECT. Pappa et al. reported a lactate sensor based on an electron-deficient naphthalene diimide (NDI) copolymer [Fig. 3(a)],104) in which the enzyme was immobilized through interactions with the ethylene glycol side chains. This provides good electrochemical contact with the redox-active copolymer, allowing electrons generated during the enzymatic reaction to be transferred to the polymer backbone and change its conduction properties. This device can detect metabolites, such as lactate, with high sensitivity and low power consumption. In particular, the polar side chains of the conducting polymer facilitate interaction with the enzyme, enabling direct electrical detection without the need for an intermediate. In another example, composite conductive nanofiber materials were used to fabricate fiber-like OECTs, making them more suitable for wearable devices.105)

Meanwhile, Sasaki and Minami, in their mini-review, described a lactate detection method based on extended-gate transistors, which enables sensing without direct immersion of the active channel.106) In this system, lactate oxidase was immobilized on the extended gate electrode, and a solution-processable π-conjugated polymer, poly{2,5-bis

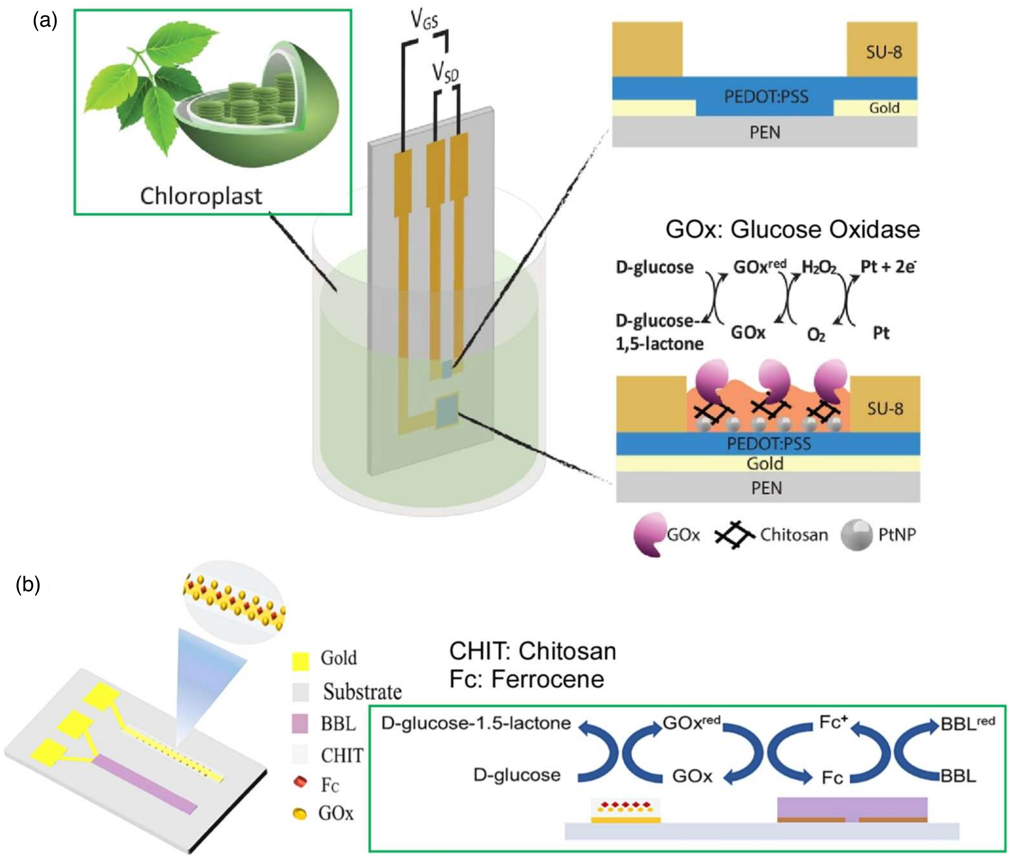

Fig. 2. Examples of glucose sensor: (a) OECT-based glucose sensor using the conducting polymer PEDOT:PSS with the gate electrode functionalized with platinum nanoparticles and glucose oxidase enzyme. Reprinted with permission from Ref. 98 Copyright 2020 Wiley-VCH; (b) OECT glucose sensor based on poly(benzimidazobenzophenanthroline) (BBL) as the n-type polymeric semiconductor channel material with immobilizing glucose oxidase and ferrocene on the gate electrode. Reprinted with permission from Ref. 99. Copyright 2024 Elsevier.

(3-alkylthiophen-2-yl)thieno[3,2-b]thiophene} (PBTTT), was used as the channel material (Fig. 3(b)). During the OFET operation, the gate voltage was applied via a reference electrode (Ag/AgCl). Both the extended gate electrode and the reference electrode were immersed in the analyte solution (e.g. body fluid), and the potential difference was measured at the interface between the sensing electrode and the analyte solution. The addition of lactate to the solution triggered an enzymatic reaction that induced electron transfer, thereby changing the surface potential of the sensing gate electrode and resulting in variations in the drain current and threshold voltage.

2.2. Sensor for biopolymer

2.2.1. DNA/RNA sensor. DNA and RNA are essential macromolecules of the human body. They serve as the foundational basis for storing, transcribing, expressing and regulating genetic information, and play crucial roles in all life-sustaining processes. These two molecules were detected using single-stranded DNA (ssDNA) as a sensing element. When ssDNA binds complementarily to target ssDNA, double-stranded DNA is formed, causing change in the gate potential and channel current. Li, Chen, Wang and co-workers developed an ultrasensitive, label-free DNA detection method using a solution-gated graphene transistor functionalized with carbon quantum dots [Fig. 4(a)].[107] The carbon quantum dots were immobilized on the gate electrode surface via mercaptoacetic acid containing a thiol group, and ssDNA probes were attached through strong π–π interactions. Upon hybridization with complementary ssDNA, double-stranded DNA is formed and subsequently detaches from the carbon quantum dot surface, resulting in a Dirac voltage shift and a corresponding channel current. The method achieved a low detection limit of 1 aM, enabling discrimination of single-base mismatches.

Zhang, Yang, Li and co-workers also reported on a solution-gated graphene transistor biosensor for the ultra-sensitive and rapid quantitative detection of microRNA-21 (miRNA-21), an early-stage prostate cancer biomarker [Fig. 4(b)].[108] A ssDNA probe designed to specifically bind the miRNA-21 molecular target was immobilized on a gold gate, where it effectively hybridized with the target, inducing a voltage shift. Because miRNA-21 molecules are electronegative due to their phosphate backbone, hybridization with the ssDNA probe corresponds to an offset voltage applied at the gate electrode. The device also exhibited a low detection limit of 1 aM and single-base mismatches were clearly distinguishable.

2.2.2. Protein sensor. Proteins are among the key macromolecules of life, and measuring protein concentration is essential for medical diagnosis, biological therapy and prevention of related diseases. The detection of proteins using OECT-based biosensors typically relies on antigen–antibody interactions, in which either antibodies or antigens are immobilized on the gate or channel of an OECT as biorecognition molecules. Yan et al. immobilized the spike protein (antigen) of severe acute respiratory syndrome coronavirus 2 (SARS-CoV-2) on the gate surface, enabling the detection of SARS-CoV-2 immunoglobulin G (IgG)

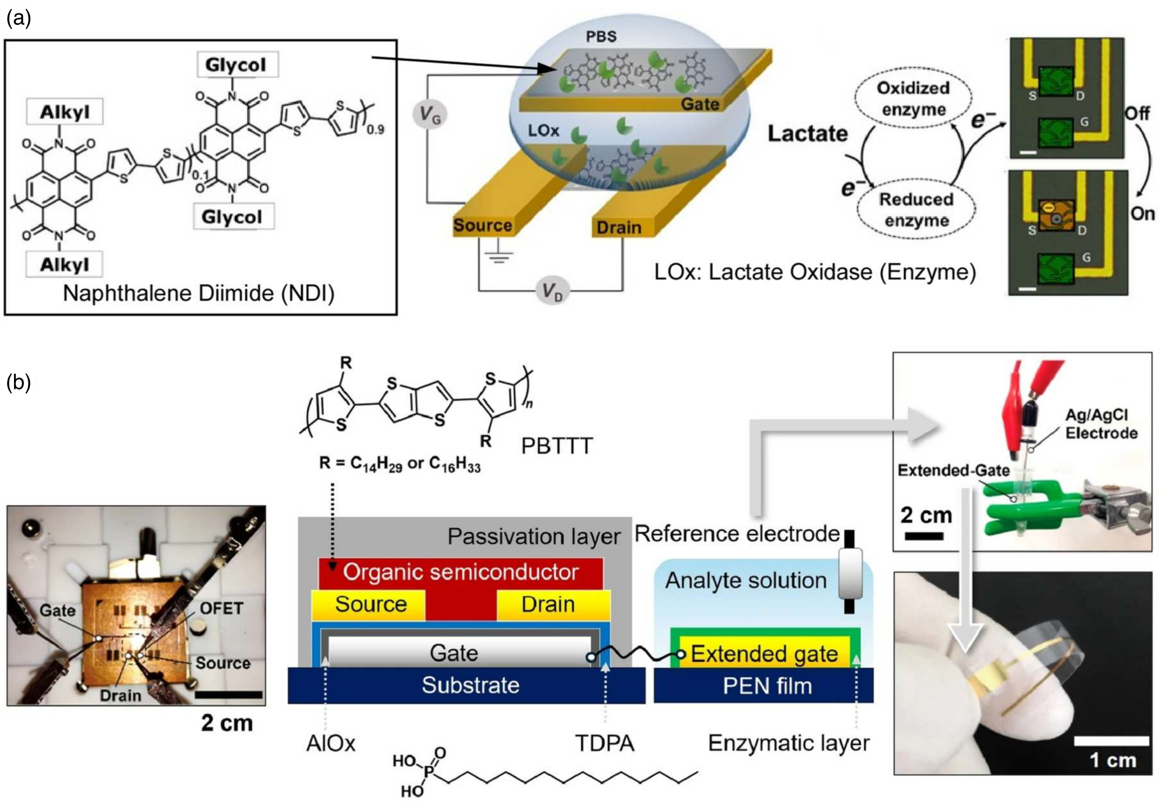

Fig. 3. Examples of lactate sensor: (a) OECT lactate sensor using an electron-deficient naphthalene diimide (NDI) copolymer, allowing electrons generated during the enzymatic reaction (lactate oxidase) to be transferred to the polymer backbone and change its conduction properties. Reprinted with permission from Ref. 104. Copyright 2018 AAAS; (b) lactate sensor using a solution-processable π-conjugated polymer material (poly{2,5-bis(3-alkylthiophen-2-yl)thieno[3,2-b]thiophene} (PBTTT) as organic semiconductor layer, where addition of lactic acid to the aqueous solution induced an enzymatic reaction resulting in electron transfer causing a change in the surface potential of the sensing gate electrode. Reproduced under terms of the CC-BY license Ref. 106. 2025 Springer-Nature.

through antigen–antibody interactions [Fig. 5(a)].[109] Because proteins composed of zwitterionic amino acids carry net charges depending on pH, changes in the local ionic concentration and distribution near the gate modulate the electrical characteristics of OECT, thereby enabling detection. By optimizing the ion concentration and pH of the test solution, they achieved a detection range from 10 fM to 100 nM (covering the SARS-CoV-2 IgG concentration range in human serum) and enabling specific detection within minutes.

The detection of human epidermal growth factor receptor 2 (HER2), an important prognostic biomarker for breast cancer, has also been reported. Yang et al. fabricated an HER2 sensor by using PEDOT:PSS as a conductive polymer and immobilizing an anti-HER2 antibody on the gate electrode.[111] This protein sensor was capable of detecting HER2 at concentrations as low as 10^{-14} g ml^{-1}, which is several orders of magnitude lower than the detection limits of previously reported electrochemical methods. Furthermore, the device could reliably distinguish between breast cancer cells and normal cells over a wide range of concentrations.

Wang et al. developed a sensor for the detection of survivin protein, a human gene product found in cancer cells [Fig. 5(b)].[110] In this sensor, the gate electrode was first functionalized with mercaptoacetic acid, followed by immobilization of anti-survivin antibodies. The authors fabricated an ultrathin, micropatterned MXene/PEDOT:PSS-based OECT biosensor, which enabled the detection of survivin protein at concentrations as low as 10 pg ml^{-1} in the OECT electrolyte. A comparison with a commercially available enzyme-linked immunosorbent assay kit showed good linearity in detection response.

Although these represent only a small subset of the potential applications, organic semiconductors have been shown to enable the detection of biomolecules spanning a wide range of molecular sizes. These findings highlight their considerable potential to contribute to the development of next-generation biosensing devices. To further advance this field, it is essential to establish more sophisticated nanoarchitectonics designs of device materials and structures. The following sections will discuss the nanoarchitectonics of organic semiconductors in terms of material fabrication, structural control and doping control.

3. Nanoarchitectonics for bio-relevant organic semiconductor devices

In the previous section, we presented several examples of biosensors to illustrate how devices based on organic polymer semiconductors and conducting polymers can interact with biological systems. These examples strongly indicate that such devices could play a crucial role in various bioprocesses. However, realizing more rational device designs will require multifaceted structural control and the integration of multiple fabrication processes. Because these technologies fundamentally rely on constructing materials and devices from the nanoscale, the concept of

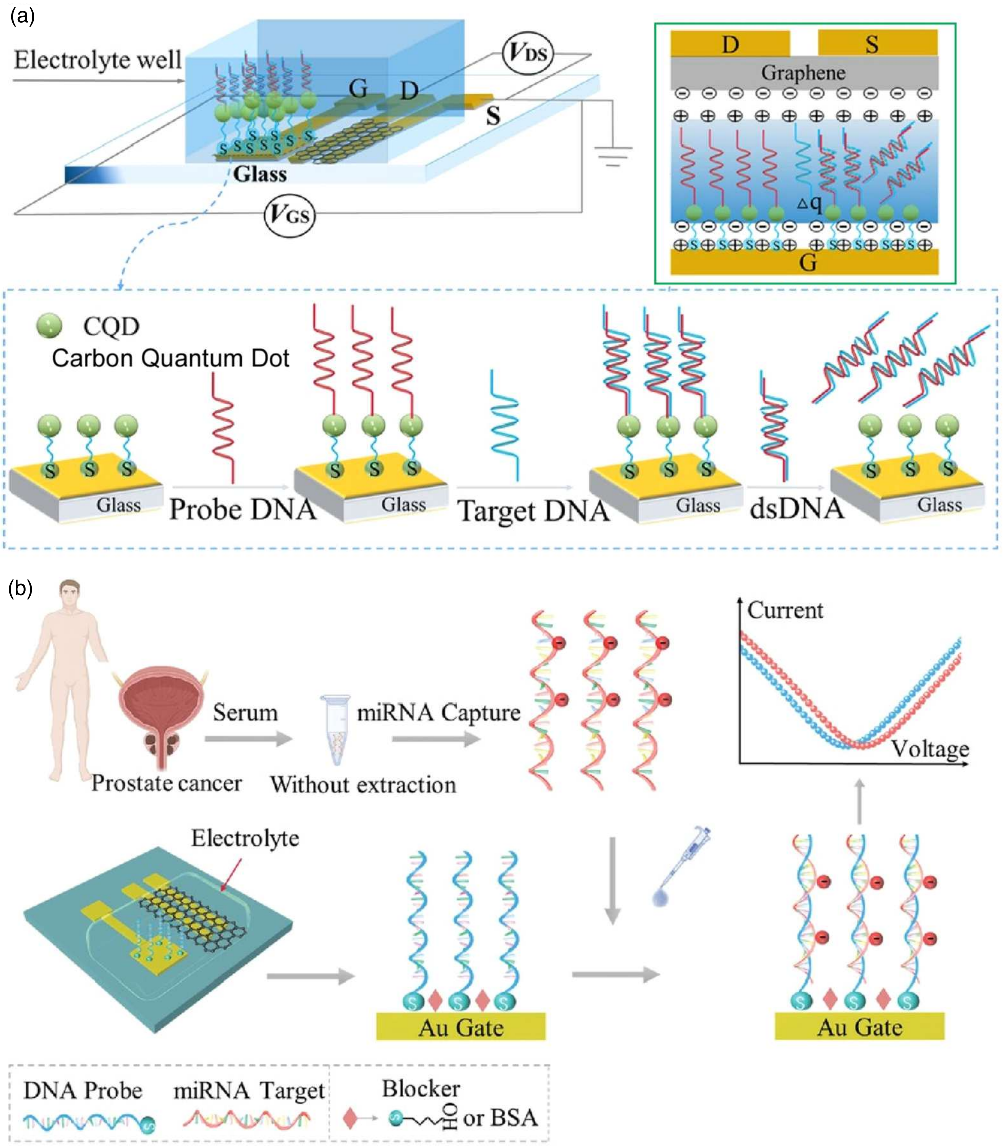

Fig. 4. Examples of DNA sensor: (a) an ultrasensitive, label-free DNA detection method using a solution-gated graphene transistor functionalized with carbon quantum dots, in which, upon hybridization with complementary ssDNA, double-stranded DNA is formed and subsequently detaches from the carbon quantum dot surface, resulting in a Dirac voltage shift and a corresponding channel current. Reprinted with permission from Ref. 107. Copyright 2022 American Chemical Society; (b) a solution-gated graphene transistor biosensor for the ultrasensitive and rapid quantitative detection of microRNA-21 (miRNA-21), an early-stage prostate cancer biomarker. Reproduced under terms of the CC-BY license Ref. 108. 2023 Wiley-VCH.

nanoarchitectonics has become increasingly important. In the following sections, we will discuss the nanoarchitectonics of organic semiconductor devices for bioprocesses applications from several perspectives.

Controlling electron transfer, electronic states and electron density is a crucial aspect in the fabrication of advanced electronic materials and devices. Certain biomaterials are capable of precisely regulating the movement of electrons and protons under ambient conditions, suggesting their potential utility in the design and fabrication of next-generation electronic systems. A representative example is the plating reaction, in which electrons are transferred among sugars, reducing agents, and metal ions to form metallic thin films. In this review, we discuss strategies for fabricating and controlling advanced nanomaterials, thin films, and devices through the use of biomolecules.

3.1. Materials nanoarchitectonics

Here, we summarize recent advances in the synthesis and assembly of conducting polymers and organic semiconductors that have been integrated into bioprocesses. In particular, the former allows in vivo synthesis, which greatly facilitates their coupling with biological systems.

3.1.1. Bio-conjugated nanoarchitectonics. Among various approaches to developing bioelectronic materials, polymeric semiconductors offer distinct advantages over their small-molecule counterparts, as they can be readily processed into uniform thin films through techniques such as spin coating. However, oxidative polymerization—commonly employed for the synthesis of polymeric semiconductors and conducting polymers—often requires heavy-metal catalysts, which can limit their applicability due to metal-induced biotoxicity. In contrast, enzymatic oxidative polymerization provides superior biocompatibility and enables highly selective and controllable polymer growth owing to the intrinsic reaction specificity of enzymes. For example, the peroxidase-mediated oxidation and polymerization of monomers containing 2,5-bis(2,3-dihydrothieno

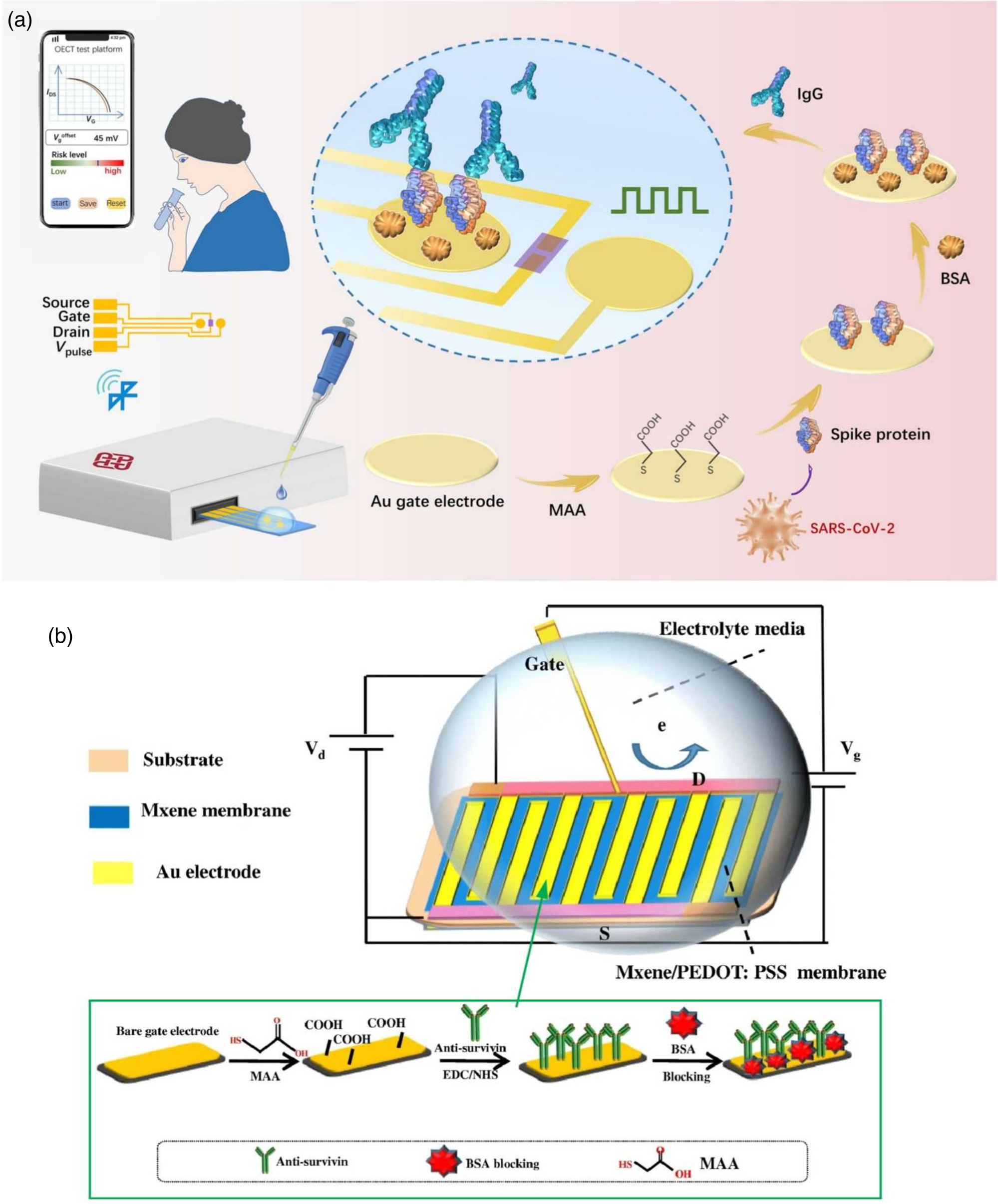

Fig. 5. Examples of protein sensor: (a) OECT-based biosensors upon antigen–antibody interactions, in which immobilization of the spike protein (antigen) of severe acute respiratory syndrome coronavirus 2 (SARS-CoV-2) on the gate surface enables the detection of SARS-CoV-2 immunoglobulin G (IgG) through antigen–antibody interactions. Reproduced under terms of the CC-BY license Ref. 109. 2021 AAAS; (b) a sensor for the detection of survivin protein, a human gene product found in cancer cells, which enabled the detection of survivin protein at concentrations as low as 10 pg ml^{-1} in the OECT electrolyte. Reprinted with permission from Ref. 110. Copyright 2021 Springer-Nature.

[3,4-b][1,4]dioxin-5-yl)thiophene (ETE) have been reported as a nanoarchitectonics-based strategy for developing in vivo device materials, as illustrated below.

Building upon this concept, Strakosas, Berggren and coworkers reported a method to induce enzymatic polymerization using endogenous metabolites, enabling the formation of flexible and highly conductive organic polymer gels directly within target tissues [Fig. 6].112) They developed a complex precursor system that contains an oxidase producing hydrogen peroxide in vivo, a peroxidase catalyzing oxidative polymerization, a water-soluble conjugated monomer, a cross-linked polyelectrolyte, and a surfactant. This hybrid system successfully induced polymerization and subsequent gelation in vivo in living organisms such as zebrafish and leeches, resulting the direct formation of flexible, conductive electrodes compatible with neutral tissue. Unlike conventional solid electrodes, this approach integrates biocompatibility with dynamic adaptability, making it highly promising for the development of implantable electronic devices and neural stimulation technologies. Importantly, it enables the creation of organic electronic gels without rigid substrate materials, which are inherently incompatible with biological tissues. The technology offers biocompatibility and dynamic adaptability not achievable with conventional solid electrodes, highlighting its potential for implantable bioelectronics and neurostimulation. Moreover, it represents a nanoarchitectonics approach for establishing a seamless interface between biological environments and electronic materials.

Similarly, expanding the concept of enzymatic in vivo polymerization to the plant kingdom, Stavrinidou et al. demonstrated that a conjugated oligomer called ETE-S can

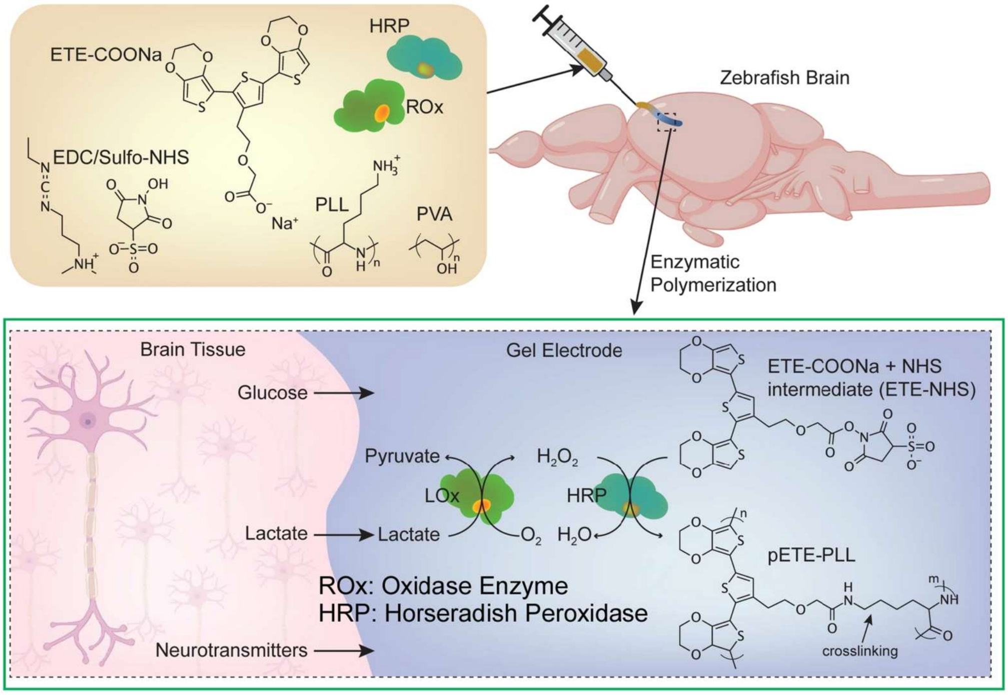

Fig. 6. A method to induce enzymatic polymerization using endogenous metabolites, enabling the formation of flexible and highly conductive organic polymer gels directly within target tissues. Reprinted with permission from Ref. 112. Copyright 2023 AAAS.

undergo in vivo polymerization into conductive polymers within plant vascular tissues through peroxidase- and hydrogen peroxide-mediated catalytic reactions.113) This approach exploits intrinsic biological metabolic build conductive structures in vivo, representing a nanoarchitectonics strategy for bridging living systems with electronic functionality. In future, the precise design of molecular backbones and side-chain structures may open new possibilities for controlling specific polymerization pathways within living organisms.

Extending this idea further to the cellular and genetic level, a single-enzyme-mediated polymerization can also be designed using chemically modified monomers whose polymerization is induced by enzymes expressed in specific cell types. This approach enables the chemical assembly of functional materials within living cells, tissues, and organisms by targeting specific genes and exploiting their genetic information. Liu et al. integrated genetic engineering with polymer chemistry to directly utilize complex cellular architectures for the in vivo synthesis of bioelectronic materials (Fig. 7).114) By inducing material synthesis in genetically targeted cells, the polymerization proceeds with high precision and selectivity at the cellular level, allowing the localized generation of functional materials within biological environments. Using this strategy, artificial enzymes expressed in specific neurons enabled the in vivo formation of conductive polymers within the neural tissue of freely moving animals. In addition, by designing genetically or anatomically targeted monomers and enzymatic catalysts, and by tuning biochemical parameters such as pH, light, and redox potential, it becomes possible to selectively trigger reactions within cells. This nanoarchitectonics concept provides a generalizable platform that extends beyond oxidative polymerization, offering a promising route for constructing cell-specific functional structures through controlled chemical synthesis.

These examples demonstrate the in vivo construction of conductive polymers aiming to integrate biological systems and electronic devices at the materials level. Such intracellular nanoarchitectonics is expected to provide an effective approach for developing direct bio-monitoring devices.

3.1.2. Interfacial nanoarchitectonics. The above describes innovative processes, such as the in vivo creation of conductive polymers, in great detail. However, nanoarchitectonics processes can also be developed by building on existing knowledge to induce innovative improvements to commonly used techniques. For instance, useful devices structures can be realized, such as highly oriented thin films of polymer semiconductors. Relevant recent examples are shown below.

As mentioned above, polymeric semiconductors can readily be fabricated into thin films using methods such as spin coating. However, due to their strong intermolecular interactions, they tend to aggregate easily, and high-temperature dissolution and processing are therefore often required. Furthermore, technologies for controlling their main-chain orientation are still under development. In contrast, many biomolecules exhibit self-organizing behavior at room temperature at hydrophilic/hydrophobic interfaces. For instance, molecular mobility is higher at air–liquid interfaces than in the solid state because molecules are confined to two-dimensional space, which facilitates orientational control. We have reported a low-energy main-chain orientation technique that exploits air–liquid and hydrophilic/hydrophobic interfaces, which are commonly encountered in the fabrication of biomimetic membranes.

Ito et al. demonstrated that uniaxial orientation along the polymer main-chain direction can be achieved using the

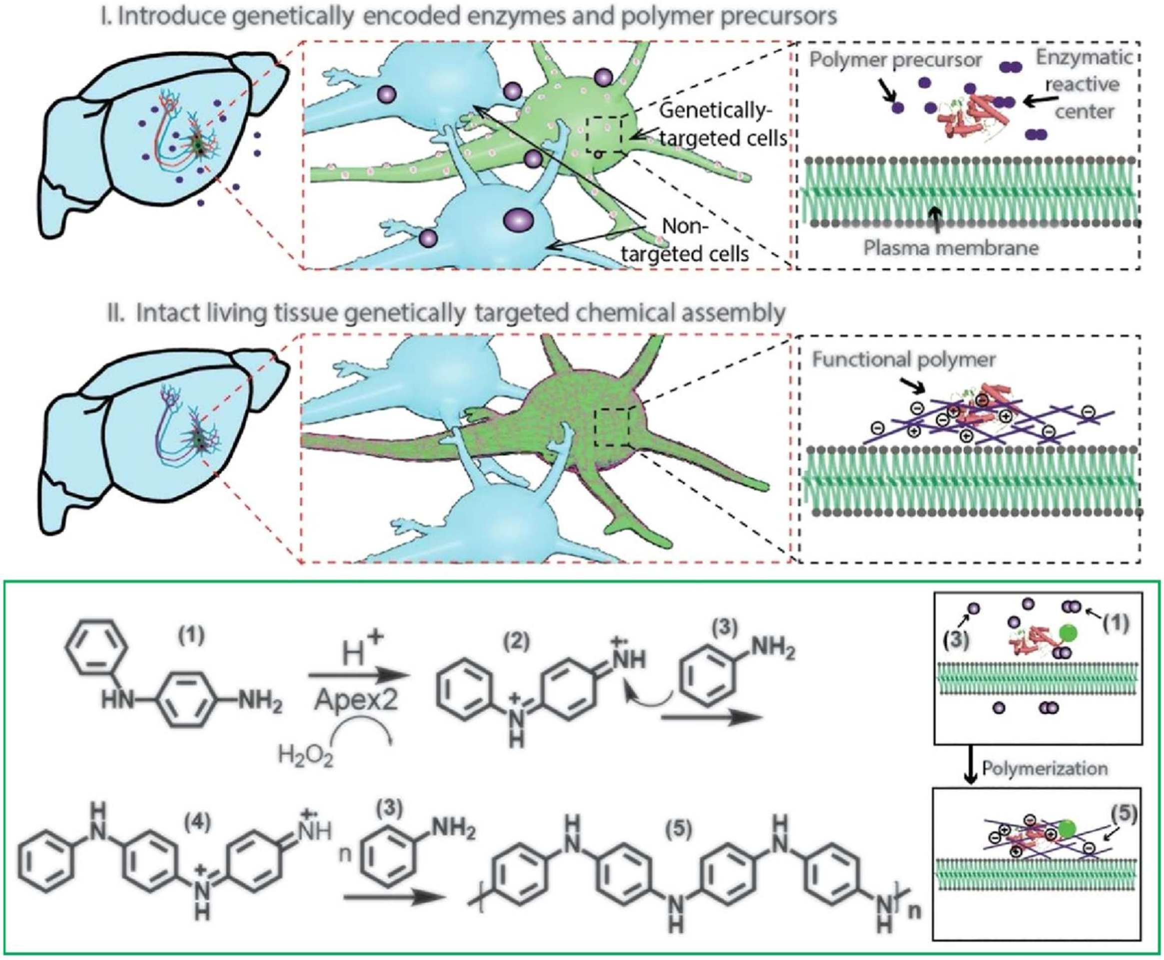

Fig. 7. Genetically targeted chemical assembly of functional materials in cells; (a) enzyme-catalyzed functional polymerization in brain (top) and reaction of Apex2-mediated polymerization from precursor reagents containing aniline monomer-dimer mixture (bottom). Reprinted with permission from Ref. 114. Copyright 2020 AAAS.

Langmuir–Blodgett (LB) technique on a heated liquid surface (Fig. 8).[115,116] This approach creates thermodynamically favorable conditions at the air–water interface, allowing nanoscale molecular aggregates to be manipulated with micrometer- to millimeter-scale dynamics. Although aqueous subphases are typically used, they are limited in both usable temperature and compatible coating materials. In this study the aqueous subphase was replaced with ethylene glycol, enabling the fabrication of ultrathin films at temperatures up to 100 °C. Ethylene glycol remains in a viscous liquid state over a wide temperature range, which allowed LB films of PBTTT, a benchmark semi-crystalline polymer semiconductor, at 100 °C. The resulting PBTTT LB films exhibited uniaxial backbone alignment and anisotropic charge transport, yielding FETs with a turn-on voltage of 0 V, a on/off ratio exceeding 10^6, and negligible hysteresis. These characteristics indicate that external factors such as residual solvent, carrier trapping, and film inhomogeneity have minimal impact. The high-temperature LB method thus enables precise control of polymer backbone orientation and can be extended to a wide range of coating materials, including those that aggregate in water at room temperature, by selecting appropriate non-aqueous subphases such as ionic liquids and diols.

More recently, Fujioka et al. reported a room-temperature process that aligns polymer main chain along the flow of hydrophilic viscous liquid (Fig. 9).[117] This approach mimics the interfacial self-organization of biomolecules and offers a promising route for precise structure control of electronic functional materials using low-energy processes. Three polymeric semiconductors—PBTTT, (poly(4,4′-bis(2-butyloctoxycarbonyl-[2,2′-bithiophene]-5,5-diyl)-alt-(2,2′-bithiophene-5,5′-diyl)), (PDCBT), and poly(3,3′′-didodecyl-2,2″:5′,2′′:5′′,2′′′-quaterthiophene-5,5′′′-diyl) (PQT)—were tested by dispensing their solutions onto glycerol circulating in a circular flow within a container, forming thin films at the air–liquid interface. To fabricate the films, a glass cylinder filled with glycerol was rotated at 20 rpm within a circular container. A droplet of PDCBT solution in a chloroform/1-chloronaphthalene mixture (the high-boiling solvent added to slow evaporation) was deposited onto the flowing glycerol surface along the cylinder's rotation path. After solvent evaporation (~5 min), ring-shaped films with uniaxially aligned main chains were obtained around the cylinder, suppressing convection effects during drying.

Polarized optical microscope and UV–vis spectroscopy confirmed the macroscopic anisotropy and uniaxial main-chain orientation of the PDCBT films. FET measurements revealed

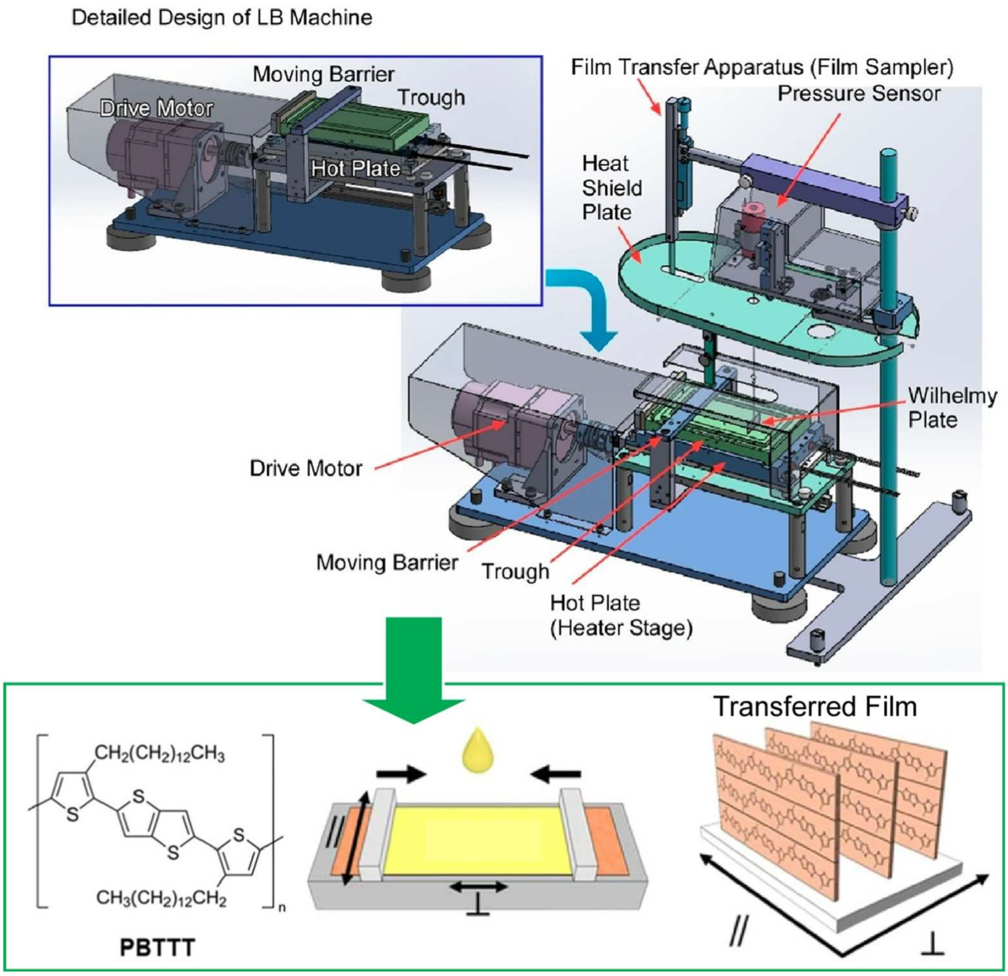

Fig. 8. Fabrication of uniaxial orientation along the polymer main-chain direction using the Langmuir–Blodgett (LB) technique on a heated liquid surface, allowing nanoscale molecular aggregates to be manipulated with micrometer- to millimeter-scale dynamics. Reprinted with permission from Ref. 115. Copyright 2020 American Chemical Society and Ref. 116. Copyright 2022 American Chemical Society.

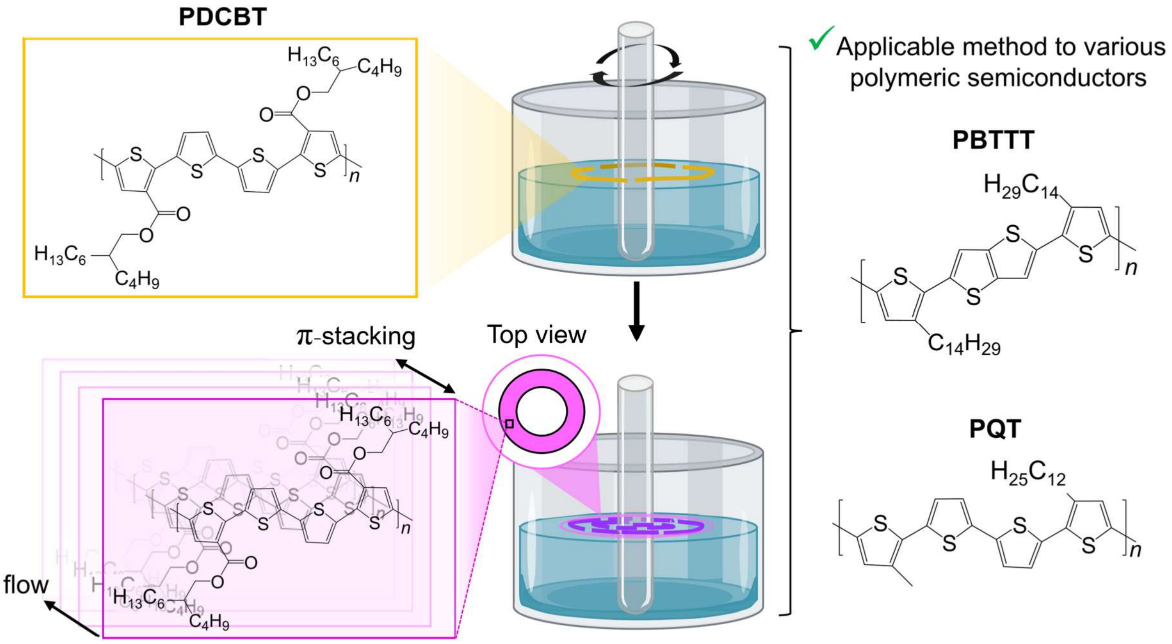

Fig. 9. A room-temperature process that aligns polymer main chain along the flow of hydrophilic viscous liquid, where three polymeric semiconductors were tested by dispensing their solutions onto glycerol circulating in a circular flow within a container, forming thin films at the air–liquid interface.

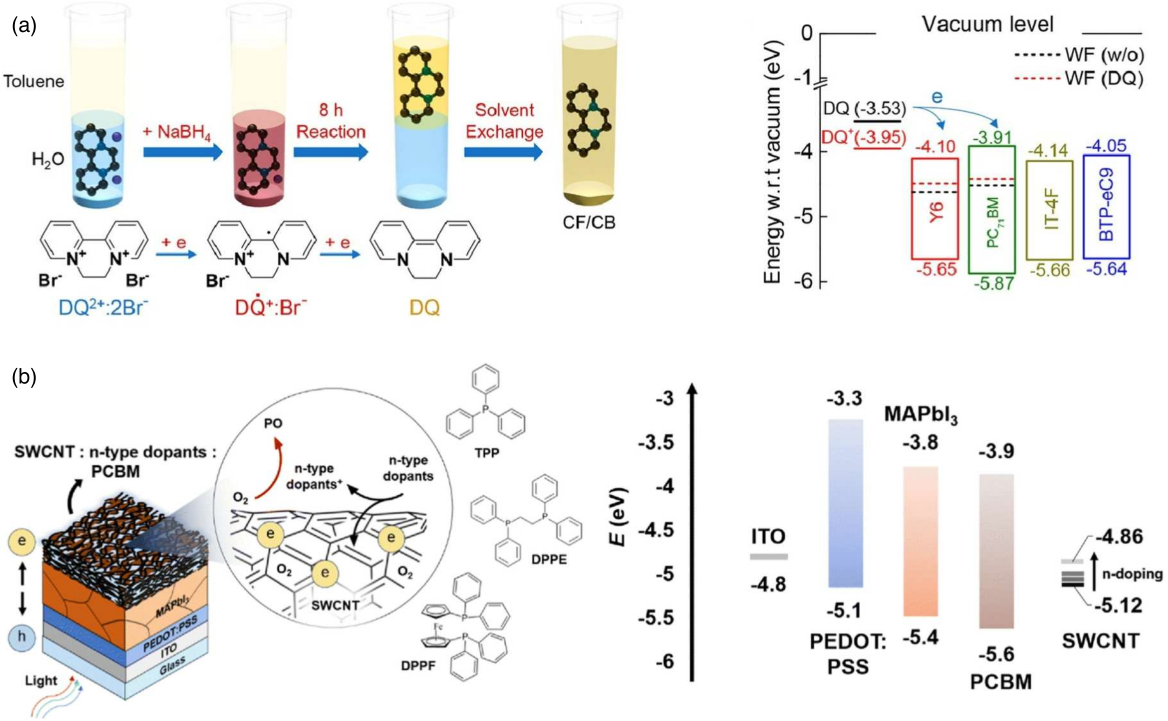

Fig. 10. (a) Performance enhancement in state-of-the-art OPVs by converting the dicationic species diquat into its neutral form and employing it as an n-type dopant. Reprinted with permission from Ref. 120. Copyright 2025 American Chemical Society; (b) molecular n-type doping strategy using organophosphorus compounds to enable SWCNTs to function as cathodes in inverted (p-i-n) PSCs. Reprinted with permission from Ref. 121. Copyright 2025 Royal Society of Chemistry.

significantly enhanced carrier transport along the flow direction, with hole mobility in the channel-parallel configuration reaching 4× that of spin-coated films. Notably, the mobility stable even after 34 d of air storage in the dark. This circular flow alignment method provides a simple, scalable approach to control molecular orientation during solution processing, where convection often disrupts alignment. By optimizing flow path designs, the technique can be scaled up, enabling the production of highly aligned polymeric semiconductor thin films for a wide range of applications.

These interfacial nanoarchitectonics techniques effectively control the orientation of polymeric semiconductor molecules, which tend to aggregate within thin films. In particular, highly oriented organic semiconductor thin films enable the fabrication of anisotropic devices. Many bioprocesses exhibit asymmetric, vectorial properties, such as unidirectional electron transport.[118,119)] Interfacial nanoarchitectonics—such as the LB method described above—provides a powerful methodology for fabricating organic semiconductor thin films that are compatible with such biosystems and coupled to bioprocesses.

3.2. Doping nanoarchitectonics

Doping is an essential process that enables the functional operation of organic semiconductors. The incorporation of dopants into the structure of organic semiconductors can be viewed as a form of molecular-level nanoarchitectonics, since it involves precise control over molecular interactions and charge transfer. Recently, bioprocesses have been proposed as an innovative route for doping, allowing the procedure to occur in aqueous environments under ambient conditions. To clarify the significance and underlying mechanism of this approach, we will first describe conventional doping methods, followed by the discussion of bioprocess-based doping in a later section.

3.2.1. Doping nanoarchitectonics, general. Doping of organic semiconductors is an essential fabrication technique, as it modulates the charge carrier density within the semiconductor and reduces contact resistance at metal-semiconductor interfaces. This technique is therefore widely applied in devices such as solar cells, thermoelectric materials, transistors, and organic light-emitting diodes (OLEDs). Representative examples are shown below.

In recent years, molecular doping has been reported to significantly enhance the operational characteristics of organic solar cells. Nugraha, Anthopoulos and co-workers achieved performance enhancement in state-of-the-art OPVs by converting the dicationic species diquat into its neutral form and employing it as an n-type dopant [Fig. 10(a)].[120)] EPR measurements confirmed the formation of free electrons in the PM6:Y6:PC71BM ternary blend. The PCE of ternary bulk heterojunction cells incorporating diquat increased from 16.7% to 17.4%. These improvements are attributed to increased absorption coefficients, balanced ambipolar transport, extended carrier lifetimes, and suppressed bimolecular recombination. These findings highlight diquat as a promising n-type dopant for realizing highly efficient stable OSCs.

n-type doping of single-walled carbon nanotubes (SWCNTs) has also been reported. Because SWCNTs typically exhibit p-type semiconductor behavior when exposed to air or oxygen, they are widely used as anodes in perovskite solar cells (PSCs). Matsuo et al. proposed a simple molecular n-type doping strategy using organophosphorus compounds to enable SWCNTs to function as cathodes in inverted (p-i-n) PSCs (glass/ITO/PEDOT:PSS/$MAPbI_3$/n-doped SWCNTs:

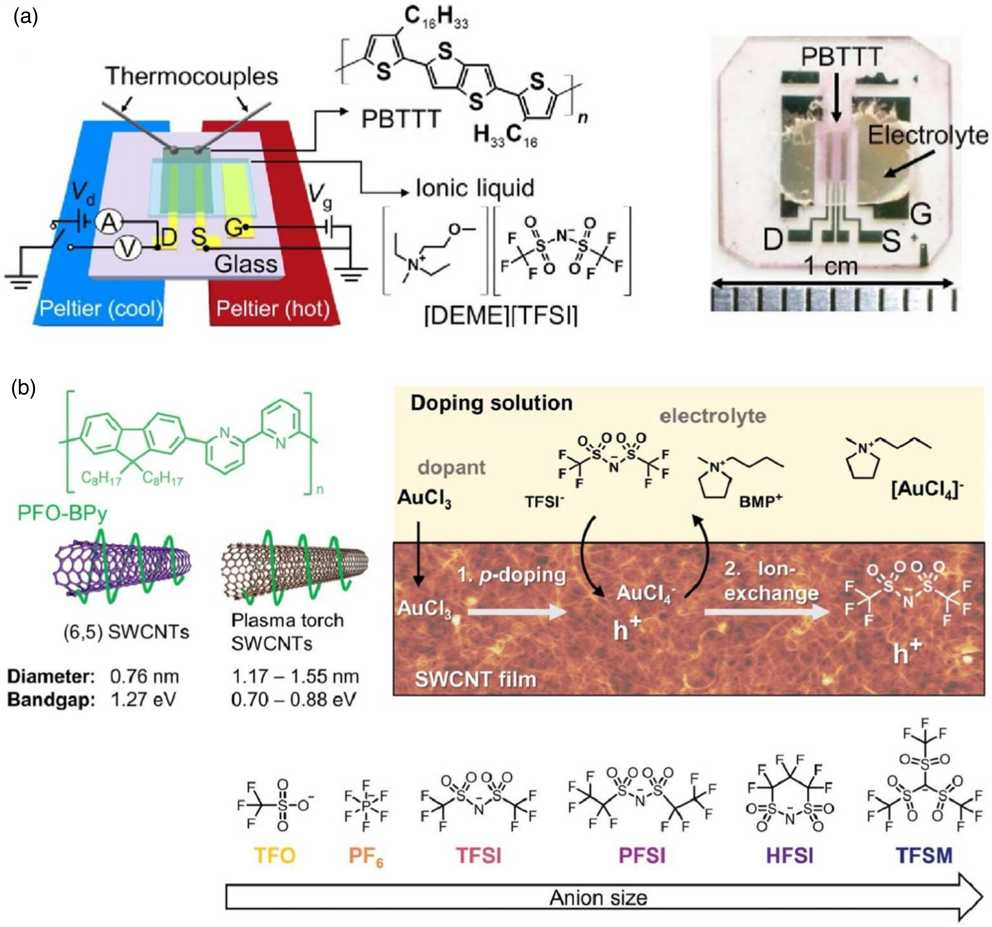

Fig. 11. (a) A schematic diagram of the experimental setup enabling simultaneous measurement of the Seebeck coefficient and electrical conductivity during carrier doping, together with a photograph of the PBTTT thin-film transistor structure. Reprinted with permission from Ref. 122. Copyright 2020 AAAS; (b) ion-exchange doping to systematically vary the size of the counterions in polymer-sorted, small- and large-diameters semiconducting SWCNT thin films, using $AuCl_3$ as the initial p-type dopant. Reprinted with permission from Ref. 123. Copyright 2024 Wiley-VCH.

PCBM) [Fig. 10(b)].[121] Among the compounds tested, the addition of 1,2-bis(diphenylphosphino)ethane (DPPE) to the SWCNT electrode increased the device efficiency from 5.1% to 8.03%. The improved stability was attributed to the hydrophobicity of the dopant, which also acted as a moisture scavenger, mitigating perovskite degradation. Overall, these findings indicate a promising avenue for the flexible and practical implementation of SWCNTs as next-generation photovoltaic electrodes.

In thermoelectric materials, p-type doping examples have been demonstrated. Conducting polymer thin films, which inherently possess structural disorder, exhibit complex electronic, transport, and thermoelectric characteristics. Owing to this disorder, the Seebeck coefficient and electrical conductivity do not exhibit a clear maximum in thermoelectric power factor upon doping, in contrast to conventional inorganic systems. However, Tanaka, Ito, Takenobu and co-workers demonstrated that a semiconducting thiophene-based polymer (PBTTT) exhibits a distinct maximum in thermoelectric power factor when subjected to wide-range carrier doping via an electrolyte gating technique using the ionic liquid N,N-diethyl-N-methyl-N-(2-methoxyethyl)ammonium bis(trifluoromethanesulfonyl)imide ([DEME][TFSI]).[122] Figure 11(a) shows a schematic diagram of the experimental setup enabling simultaneous measurement of the Seebeck coefficient and electrical conductivity during carrier doping, together with a photograph of the PBTTT thin-film transistor structure. The power facter maximum appeared near the insulator-to-metal transition, as confirmed by the temperature dependence of conductivity and magnetoresistance measurements. In the metallic regime, charge transport was found to follow the conventional Mott relation, indicating that structural disorder was effectively suppressed. These findings provide important physical insights into doping nanoarchitectonics for performance tuning of conducting polymers toward high-efficiency polymer-based thermoelectric devices for future energy harvesting applications.

To further optimize doping methods and develop better dopants, it is essential to understand the effect of dopant counterions on the charge transport and thermoelectric properties of semiconducting SWCNT networks. Zaumseil et al. used ion-exchange doping to systematically vary the size of the counterions in polymer-sorted, small- and large-diameters semiconducting SWCNT thin films, using $AuCl_3$ as the initial p-type dopant [Fig. 11(b)].[123] They investigated the impact of ion size on conductivity, the Seebeck coefficient, and the power factor. Larger anions were found to significantly increase electrical conductivity, and this effect was more pronounced in small-diameter nanotubes than in large-diameter nanotubes. Meanwhile, the position of the power-factor-versus-conductivity peak remained unchanged. Semiconducting SWCNT networks thus provide an ideal

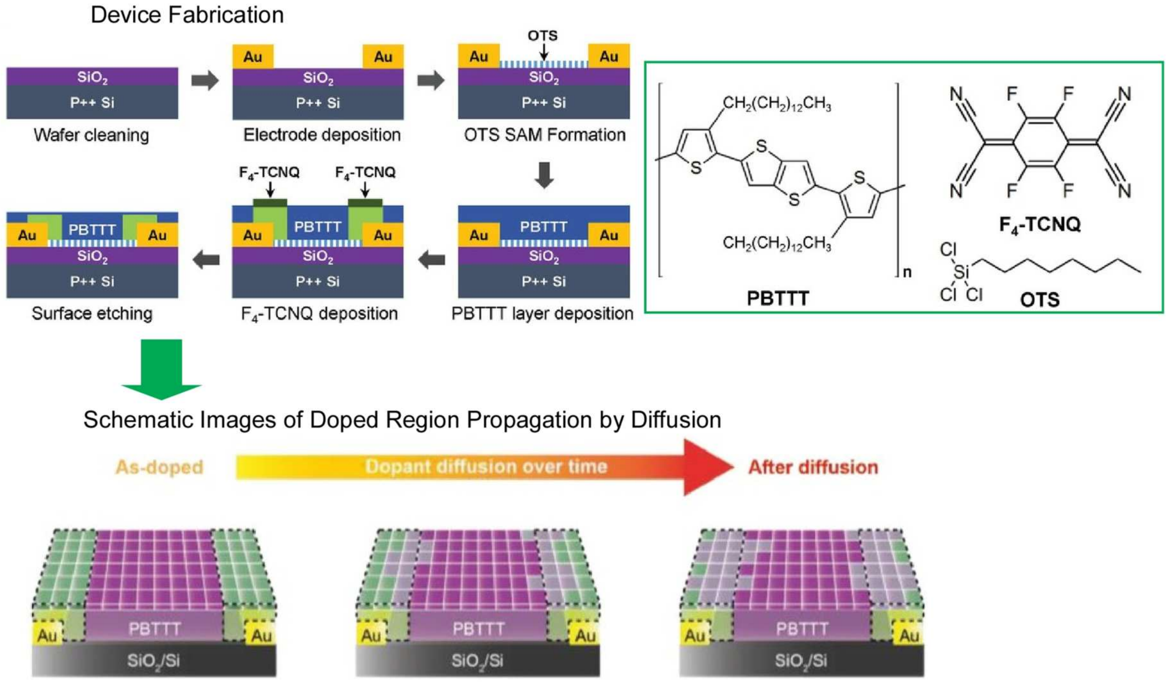

Fig. 12. Reduction of contact resistance in PBTTT-based bottom-gate OFETs by selectively evaporating 2,3,5,6-tetrafluoro-7,7,8,8-tetracyanoquinodimethane (F4-TCNQ) near the contacts, enabling its solid-state diffusion, where post-doping optimization suppressed surface dopant diffusion while maintaining high conductivity near electrodes, nearly doubling transistor current at comparable gate voltages. Reprinted with permission from Ref. 124. Copyright 2019 Wiley-VCH.

model system for investigating how different dopant counterions affect charge transport and thermoelectric properties in disordered percolating semiconductors such as conjugated polymers. These insights are expected to guide the development of dopants and doping strategies for improving thermoelectric materials.

We next discuss an example of contact resistance reduction between metals and OSCs. Schottky barriers at metal–OSC interfaces often cause non-ideal transfer characteristics in the low drain-voltage regime of OFETs. Kang, Lee, and co-workers reduced the contact resistance in PBTTT-based bottom-gate OFETs by selectively evaporating 2,3,5,6-tetrafluoro-7,7,8,8-tetracyanoquinodimethane (F4-TCNQ) near the contacts, enabling its solid-state diffusion (Fig. 12).[124) UPS measurements confirmed successful p-type doping, with the Fermi-highest occupied molecular orbital (HOMO) offset decreasing from 0.87 eV to 0.26 eV. Post-doping optimization suppressed surface dopant diffusion while maintaining high conductivity near electrodes, nearly doubling transistor current at comparable gate voltages. This molecular injection doping approach effectively addresses contact resistance issues and enables low-power organic electronics.

As a final example, we consider doping in OLEDs. The application of doping in high-performance OLEDs is limited by the challenge of p-type molecular doping of organic materials with high ionization energies. Reineke et al. demonstrated that hexacyanotrimethylenecyclopropane (CN6-CP), which has an electron affinity 0.6 eV higher than that of F4-TCNQ, can be used as a p-type dopant when mixed with the hole-injection material 4,4′-cyclohexylidenebis[N,N-bis(4-methylphenyl)benzenamine] (TAPC).[125) To investigate the dopant's function in devices, they fabricated green OLEDs with structure shown in Fig. 13. Using CN6-CP-doped TAPC, a low driving voltage of 2.92 V at a practical luminance of 1000 cd m^{-2} and 3.18 V at a current density of 10 mA cm^{-2} was achieved. These results demonstrate that dopant has great potential for future applications in organic optoelectronic devices, including both monochrome and white OLEDs.

Given the many potential applications of doped organic semiconductors, it would be highly desirable to perform doping under ambient conditions, such as in air or aqueous solution.

3.2.2. Proton-coupled electron transfer (PCET) driven nanoarchitectonics for aqueous doping.

Among the doping methods for organic semiconductors, chemical doping via redox reactions relies on electron transfer between the semiconductor and dopant molecules. Conventional solution-based chemical doping requires inert atmospheres and organic solvents to prevent unwanted side reactions with oxygen and water, hindering scalability. Since certain devices require chemical doping for optimal performance, doping method under ambient conditions are essential for large-scale fabrication. Recently, Ishii, Yamashita and co-workers achieved such doping through pH-controlled preventing unwanted redox reactions with water/oxygen.[126) This approach harnesses PCET—a bio-inspired mechanism—for precise doping control (Fig. 14). Below, we detail PCET principles, mechanisms, applications, and prospects. PCET represents a core mechanism in biological energy conversion and enzymatic reactions, involving the concerted or sequential transfer of protons and electrons. In biological systems—operating under ambient aqueous conditions—PCET plays a critical role in photosynthesis, cellular respiration, enzymatic catalysis, and ATP synthesis. By

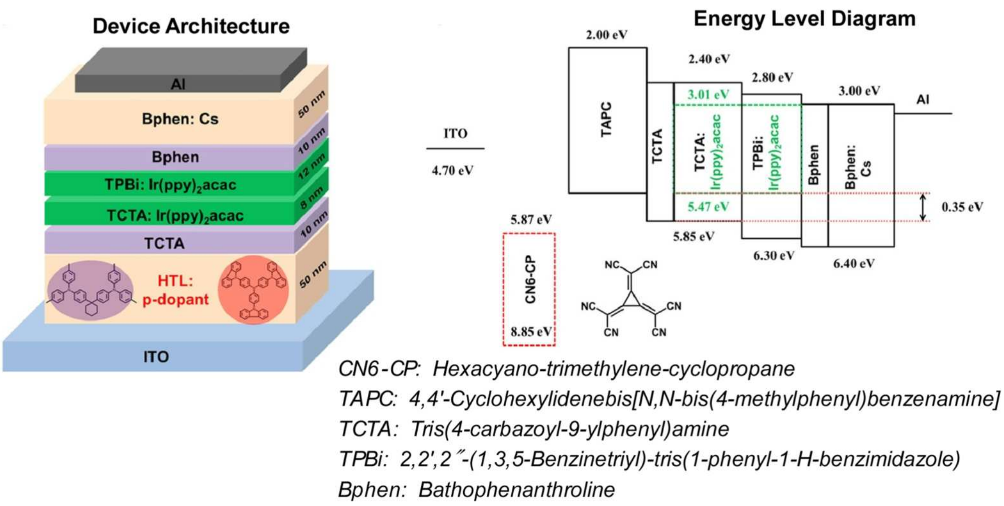

CN6-CP: Hexacyano-trimethylene-cyclopropane
TAPC: 4,4'-Cyclohexylidenebis[N,N-bis(4-methylphenyl)benzenamine]
TCTA: Tris(4-carbazoyl-9-ylphenyl)amine
TPBi: 2,2',2″-(1,3,5-Benzinetriyl)-tris(1-phenyl-1-H-benzimidazole)
Bphen: Bathophenanthroline

Fig. 13. Investigation on the dopant's function in devices using green OLEDs. Reprinted with permission from Ref. 125. Copyright 2019 American Chemical Society.

integrating PCET into organic semiconductor chemistry, air- and aqueous-compatible chemical doping becomes feasible. A key advantage of PCET lies in its Nernstian response, enabling precise control of redox potentials via proton activity—a parameter adjustable over more than 10 orders of magnitude. In this paper's system, they utilize the two-electron, two-proton PCET reactions of the benzoquinone/hydroquinone (BQ/HQ) redox couple to control p-type doping efficiency in aqueous solution. Indeed, decreasing solution pH systematically increases electrical conductivity, confirming effective doping.

The assumed mechanism of this doping process is proposed as follows. Hole injection into the organic semiconductor proceeds via the pH-dependent PCET reaction of BQ/HQ. Dopant anions then intercalate into the organic semiconductor thin film, compensating the injected holes. These processes occur either sequentially or concertedly, enabling anion species Y^- doping into PBTTT films without compromising crystallinity. The synergistic interplay between PCET and anion intercalation allows optimization of doping efficiency, stability, and electronic properties through rational dopant anion selection. Notably, conductivity measurements demonstrate highly efficient p-type doping only when both BQ and dopant salts are present. PBTTT films achieved conductivities as high as ~180 S cm^{-1} when combined with LiNFSI. Using large, non-nucleophilic anions further enhances air-stability of the p-doped films.

Doping with PCET has also been successfully applied to other systems. Rodríguez-Martínez et al. demonstrated that PCET using BQ as the oxidant and lithium bis(trifluoromethylsulfonyl)imide (Li-TFSI) as the counterion is highly suitable for p-type doping of polymer-sorted semiconducting SWCNT networks (Fig. 15).[127] The doping level can be precisely tuned by pH, enabling optimization to the power factor peak position. For narrow-bandgap SWCNTs, PCET doping achieves thermoelectric power factors equivalent to conventional methods. Moreover, PCET-doped SWNTs exhibit superior long-term stability, maintaining electrical conductivity for at least 5 d in air—significantly outperforming three other methods, including $AuCl_3$-based ion-exchange doping. These results confirm PCET as a key technique for p-type doping of flexible, high-performance semiconducting SWNT networks in thermoelectric applications.

This PCET-based chemical doping method offers unprecedented controllability, stability, scalability, and versatility across diverse structures through simple solution processing. It unlocks diverse possibilities for advanced organic semiconductor devices. The demonstrated PCET route will accelerate manufacturing of high-performance, reliable devices, including sensors and bioelectronics. Compared to conventional vacuum- or inert-atmosphere-based methods in organic solvents, this doping nanoarchitectonics approach exhibits superior scalability, stability, and tunability. As a room-temperature semiconductor process and platform for biomolecular electronics, it holds immense potential for next-generation flexible electronics and beyond.

3.2.3. Bio-pathway nanoarchitectonics for sugar redox driven doping.

For n-type chemical doping, the HOMO of the reductant must be shallower than the semiconductor's lowest unoccupied molecular orbital (~-4.0 eV versus vacuum).[128] However, shallow-HOMO reductants are readily deactivated by dissolved oxygen (O_2: -5.26 eV versus vacuum),[129] making n-type doping more challenging than p-type. While strong, moderately stable n-type doping has been achieved in gloveboxes using dimer dopants,[130] catalytic reactions,[131] and ion-exchange methods,[132,133] ambient n-type doping remains unreported. Recently, Ohashi, Yamashita and co-workers achieved n-type doping of organic semiconductors using a biochemical pathway (Fig. 16).[134] This study employs a reductant with sufficient reducing power and stability in air, paired with redox mediators to efficiently extract electrons. Redox reactions mediated by such mediators are ubiquitous in biology. Bio-mimetic strategies thus enables redox potential control while suppressing oxygen-induced degradation.

A polymer thin film of PNDI(2HD)T—comprising naphthalene-1,4:5,8-bis(dicarboximide) (NDI) with branched alkyl chains and thiophene units—employed as the organic semiconductor. This polymer semiconductor thin film was then immersed in an aqueous doping solution containing fructose, flavin mononucleotide (FMN) and bulky molecular

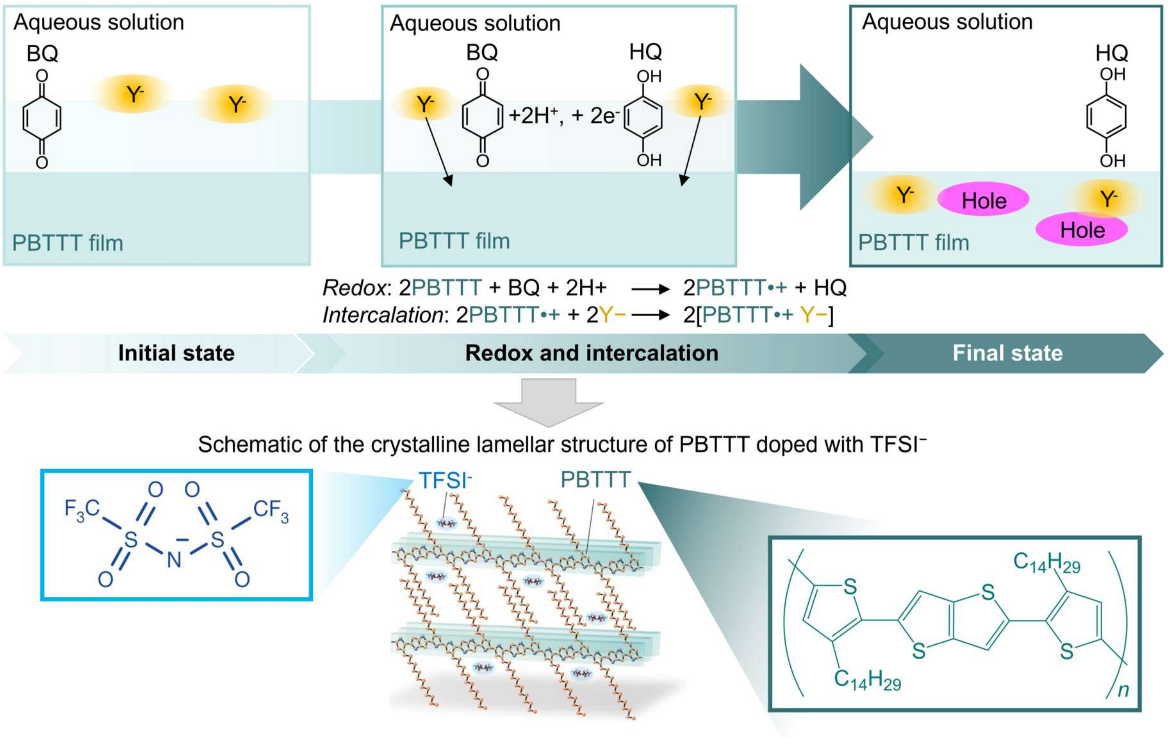

Fig. 14. Doping of organic semiconductor films through proton-coupled electron transfer (PCET) in which the two-electron, two-proton PCET reactions of the benzoquinone/hydroquinone (BQ/HQ) redox couple to control p-type doping efficiency in aqueous solution.

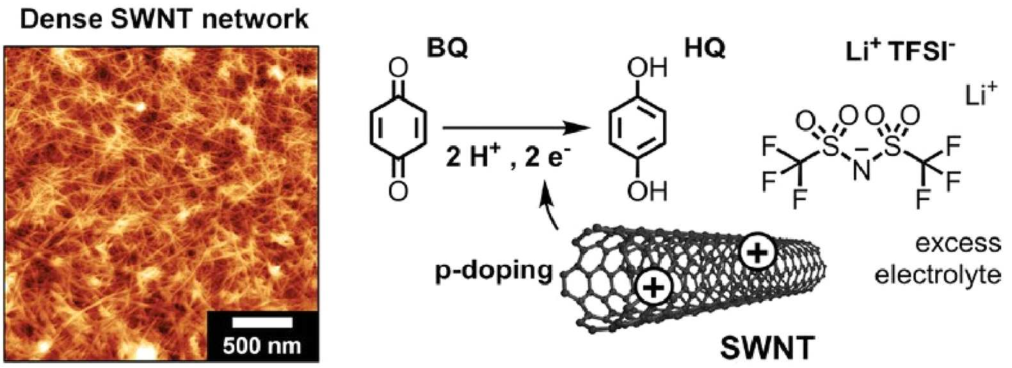

Fig. 15. PCET-based doping of polymer-sorted semiconducting SWCNT networks using BQ as the oxidant and lithium bis(trifluoromethylsulfonyl) imide (Li-TFSI) as the counterion. Reproduced under terms of the CC-BY license Ref. 127. 2025 Wiley-VCH.

cations. During this process, electrons were transferred from the fructose to the FMN, and then from the FMN to the organic semiconductor thin film. These electrons were compensated for by introducing bulky molecular cations into the thin film, which were selected to improve the stability and transport properties of the carriers. This process increased the conductivity of the thin film from less than 10^{-9} S cm^{-1} to 4×10^{-4} S cm^{-1}, confirming successful n-type doping. While fructose provides environmental stability through slow redox kinetics, its reducing capability is limited. Using an FMN redox mediator accelerated the redox reaction rate and achieves n-type doping. The doped organic semiconductor thin films exhibited conductivities exceeding 10^{-3} S cm^{-1} at room temperature, as well as long lifetimes in air. Owing to the thermal stability of the material, facile thin-film encapsulation realized a lifetime of 25 h at 100 °C in air, which is remarkable considering the shallow IP of around 3.8 eV for the doped PNDI(2HD)T.

Solution processing of organic semiconductors enables convenient fabrication of doped thin films, paving the way for printed electronics. This study demonstrates that n-type doping—previously confined to glovebox conditions—can now be achieved under ambient conditions using aqueous solutions. These results suggest that room-temperature p- and n-type doping will enable advanced organic devices for thermoelectric generators, and stable low-work-function electron transport layers. Moreover, the observed biomolecule-semiconductor electron transfer opens up new avenues for energy storage, transfer, and conversion.

This system represents a breakthrough by achieving n-type doping of organic semiconductors under ambient aqueous conditions. It is equally groundbreaking by incorporating biologically ubiquitous processes, such as sugar redox

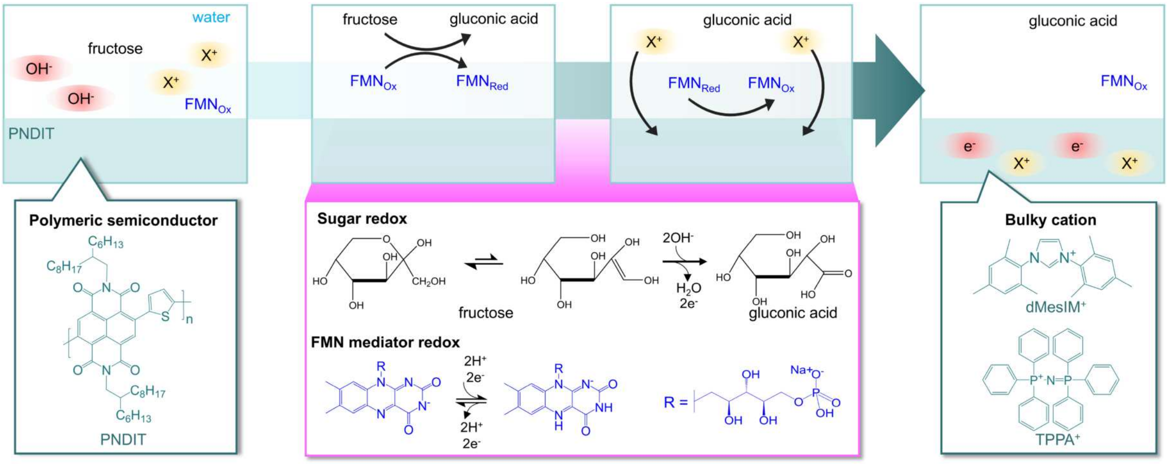

Fig. 16. A biochemical pathway of n-type doping of organic semiconductors using flavin mononucleotide (FMN), where electrons are transferred from the fructose to the FMN, then from the FMN to the organic semiconductor thin film, and electrons were compensated for by introducing bulky molecular cations into the thin film.

reactions and coenzyme mediators. Continued progress could enable seamless integration of any bioprocess into organic semiconductor devices.

3.3. Natural molecules for electrode work function engineering and device stabilization

Biomolecules have also been explored as functional components for improving the stability and environmental compatibility of organic semiconductor devices. For example, Akaike et al. reported that the adsorption of caffeic acid, a polar phenylpropanoid biosynthesized by plants, universally increases the work function of metal electrodes.135) The formation of a dipole layer arising from the oriented adsorption of caffeic acid molecules leads to a work function increase of up to 0.7 eV, enabling effective tuning of the hole injection barrier in organic electronic devices. As a result, monolayer devices incorporating a caffeic acid interlayer exhibited hole injection currents that were 10^1–10^2 larger under forward bias. These results highlight the potential of naturally occurring molecules as interfacial modifiers for controlling the electronic properties of organic semiconductor devices.

Biomolecules can also play an important role in stabilizing air-sensitive organic semiconductors. The development of n-type organic semiconductors has long been hindered by their susceptibility to degradation by oxygen and water. Li, Hu and co-workers demonstrated that vitamin C can act as an effective stabilizing agent for n-type organic semiconductors.136) Vitamin C functions as a reactive oxygen species scavenger through a cascade process involving sacrificial oxidation and triplet quenching, thereby suppressing oxidative damage and reducing electron trapping. When applied to OFETs, this strategy significantly improved both device performance and operational stability (Fig. 17). Such bio-inspired stabilization strategies may provide a general route for improving the stability of a wide range of organic electronic materials, including conducting polymers, light-emitting materials, and other emerging semiconductors.

These examples demonstrate that naturally derived molecules can serve not only as environmentally benign components but also as functional elements for controlling electronic processes in organic devices. The incorporation of biomolecules into organic semiconductor systems may therefore contribute to the development of sustainable and biocompatible electronic technologies.

4. Future perspectives

Drawing on the concept of nanoarchitectonics—the construction of functional systems from atoms and molecules—this review highlights recent advances in integrating organic semiconductors with bioprocesses. Although research in this area remains relatively young, the examples discussed here demonstrate the considerable potential of organic semiconductors to interact with biomolecular systems and to serve as platforms for bio-integrated electronic devices.

Biosensors represent a particularly important intersection between organic semiconductor devices and biological processes. Organic semiconductors have been shown to detect a wide range of biomolecules, from small biomolecules to large biomacromolecules, illustrating their versatility as sensing platforms. In addition, strategies such as the formation of conducting polymers within living organisms provide a promising route toward direct integration of biological systems with electronic functionality. Interfacial nanoarchitectonics, including improved LB approaches and controlled molecular alignment in thin films, offers powerful tools for constructing well-defined organic semiconductor structures compatible with biological environments.

Doping remains a central process for enabling the functionality of organic semiconductors. However, conventional chemical doping often requires inert atmospheres and organic solvents, limiting practical scalability. Bio-inspired approaches offer attractive alternatives. Processes such as PCET, which are ubiquitous in biological energy conversion systems, may enable efficient p-type doping under ambient or aqueous conditions. Similarly, bio-based strategies for n-type doping, including sugar which is stable reducing agents in air and redox mediation, demonstrate how biological concepts can expand the operational environment of organic semiconductors.

The combination of organic semiconductors with bioprocesses opens new opportunities for applications ranging from biosensing to wearable and implantable electronics. Owing to their mechanical flexibility, light weight, and

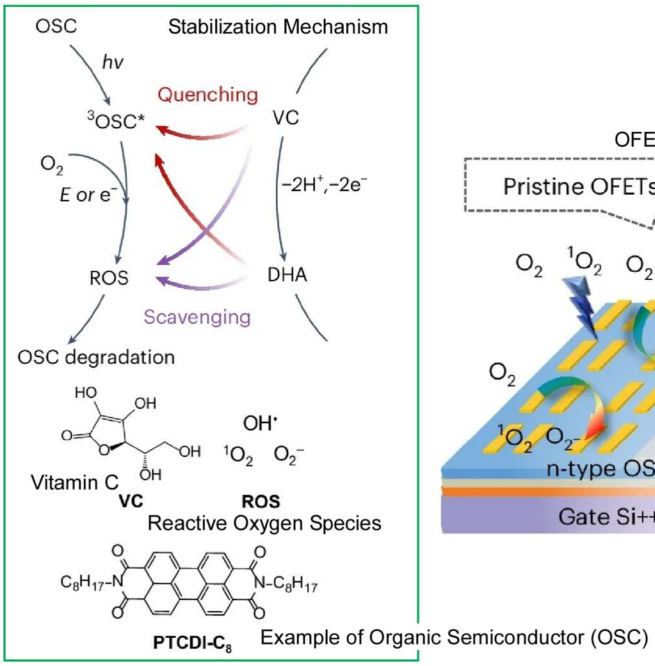

Fig. 17. Use of vitamin C as an effective stabilizing agent for n-type organic semiconductors, where vitamin C functions as a reactive oxygen species (ROS) scavenger through a cascade process involving sacrificial oxidation and triplet quenching, thereby suppressing oxidative damage and reducing electron trapping. Reprinted with permission from Ref. 136. Copyright 2024 Springer-Nature.

biocompatibility, organic semiconductor devices are well suited for seamless integration with biological interfaces. In the context of an increasingly connected IoT society, such devices could function as low-cost, flexible sensors capable of continuous physiological monitoring in healthcare and daily life.

Ultimately, the precise control over nanoscale structures will be essential for realizing the full potential of these systems. Highly controlled molecular structures not only give rise to biological functions but also suppress the formation of trap states, which pose a critical challenge to the practical implementation of organic semiconductor devices. In this context, nanoarchitectonics provides a powerful framework for the design and application of next-generation organic semiconductor biointerfaces. Continued exploration at the intersection of materials science, electronics, and biology is expected to drive the development of advanced organic semiconductor biodevices with significant technological and societal impact.

If we further consider key real-world implementation challenges in practical usages, more fundamental matters becomes crucial. It is essential to focus on improving fundamental performance tailored to practical applications, such as long-term and operational stability, resistance to various environments—including underwater conditions—and cost-effectiveness that allows for single-use disposal. For example, steady researches are underway on topics such as the selection of organic semiconductors and dopants with appropriate film constructions to achieve long-term stability[137] and operational stability.[138] Furthermore, by developing devices that operate at the single-molecule-layer level, the amount of material used can be drastically reduced, thereby alleviating cost concerns. In short, while pursuing cutting-edge research is important, thoroughly investigating fundamental aspects such as stability may be the major challenge that paves the way for realistic applications.

Acknowledgments

This work was supported in part by JSPS KAKENHI grants (Nos. JP23H05459, JP25H00898) and JST FOREST (JPMJFR236R).

---

1) G. Povie, Y. Segawa, T. Nishihara, Y. Miyauchi, and K. Itami, Science **356**, 172 (2017).
2) M. Sugiyama, M. Akiyama, Y. Yonezawa, K. Komaguchi, M. Higashi, K. Nozaki, and T. Okazoe, Science **377**, 756 (2022).
3) T. Mita, Bull. Chem. Soc. Jpn. **98**, uoaf028 (2025).
4) H. Oguri, Bull. Chem. Soc. Jpn. **98**, uoaf036 (2025).
5) T. Nakamura et al., Nat. Commun. **11**, 3008 (2020).
6) X.-L. Pei, P. Zhao, H. Ube, Z. Lei, M. Ehara, and M. Shionoya, Nat. Commun. **15**, 5024 (2024).
7) S. Yasumura and K. Shimizu, Bull. Chem. Soc. Jpn. **98**, uoaf080 (2025).
8) M. Han, T. Nagaura, J. Kim, S. M. Alshehri, T. Ahamad, Y. Bando, A. Alowasheeir, Y. Asakura, and Y. Yamauchi, Bull. Chem. Soc. Jpn. **98**, uoae136 (2025).
9) T. Yamamoto, A. Takahashi, and H. Otsuka, Bull. Chem. Soc. Jpn. **97**, uoad004 (2024).
10) R. Nagaya, T. Seko, K. Okamoto, K. Ueno, M. Atobe, and N. Shida, Nat. Commun. **16**, 10679 (2025).
11) T. Nishikawa, Bull. Chem. Soc. Jpn. **98**, uoae129 (2025).
12) M. Hollamby, H. Hanayama, and S. Yagai, Nat. Commun. **16**, 9316 (2025).
13) S. Datta et al., Nature **583**, 400 (2020).
14) H. Nabika, Bull. Chem. Soc. Jpn. **98**, uoaf048 (2025).
15) T. Maeda, N. Okamura, S. Das, T. Ishida, H. Kotera, A. Ajayaghosh, A. Saeki, and S. Yagi, Angew. Chem. Int. Ed. **65**, e16556 (2026).
16) S. Akine, Bull. Chem. Soc. Jpn. **98**, uoaf084 (2025).
17) T. Kitao, Bull. Chem. Soc. Jpn. **97**, uoae103 (2024).
18) S. Miyazaki, N. Ogiwara, C. A. Nagasaka, K. Takiishi, M. Inada, and S. Uchida, Bull. Chem. Soc. Jpn. **97**, uoae105 (2024).
19) R. Akai, S. Kitajima, K. Okubo, N. Serizawa, H. Nishihara, H. Kasai, and K. Oka, Nat. Commun. **16**, 10798 (2025).
20) K. Beamsley, N. Hosono, and T. Uemura, Nat. Commun. **16**, 6984 (2025).
21) A. Kuzume and K. Yamamoto, Bull. Chem. Soc. Jpn. **97**, uoae022 (2024).
22) G. Chen, M. Isegawa, T. Koide, Y. Yoshida, K. Harano, K. Hayashida, S. Fujita, K. Takeyasu, K. Ariga, and J. Nakamura, Angew. Chem. Int. Ed. **63**, e202410747 (2024).

23) K. Ariga, S. Akakabe, R. Sekiguchi, M. L. Thomas, Y. Takeoka, M. Rikukawa, and M. Yoshizawa-Fujita, ACS Omega **9**, 22203 (2024).
24) X. Niu and M. Kanezashi, Bull. Chem. Soc. Jpn. **98**, uoaf030 (2025).
25) B. Roy and T. Govindaraju, Bull. Chem. Soc. Jpn. **97**, bcsj20230224 (2024).
26) A. Usami et al., Science **388**, 1055 (2025).
27) T. Sugawara, M. Matsuo, and T. Toyota, Bull. Chem. Soc. Jpn. **98**, uoae134 (2025).
28) L. Sutrisno, G. J. Richards, J. D. Evans, M. Matsumoto, X. Li, K. Uto, J. P. Hill, M. Taki, S. Yamaguchi, and K. Ariga, Sci. Adv. **11**, eadz6633 (2025).
29) K. Kimura, K. Miwa, H. Imada, M. Imai-Imada, S. Kawahara, J. Takeya, M. Kawai, M. Galperin, and Y. Kim, Nature **570**, 210 (2019).
30) T. Tahara, Bull. Chem. Soc. Jpn. **97**, uoae012 (2024).
31) W. Yoshimune, Bull. Chem. Soc. Jpn. **97**, uoae046 (2024).
32) Y. Kameda, M. Kowaguchi, Y. Amo, T. Usuki, K. Nawa, and T. J. Sato, Bull. Chem. Soc. Jpn. **97**, uoae006 (2024).
33) W. Ishii and T. Nakashima, Bull. Chem. Soc. Jpn. **98**, uoaf090 (2025).
34) Y. Tomoshige, M. Tamura, and H. Ishihara, Appl. Phys. Express **18**, 022004 (2025).
35) K. Uemura and A. Takamori, Bull. Chem. Soc. Jpn. **98**, uoaf101 (2025).
36) Y. Yamada and Y. Kanemitsu, J. Phys. Chem. Lett. **16**, 4496 (2025).
37) L. Xian, X. Tian, Z. Liu, S. Liu, and J. Zhao, Bull. Chem. Soc. Jpn. **98**, uoaf009 (2025).
38) R. P. Feynman, Eng. Sci. **23**, 32 (1960).
39) M. Roukes, Sci. Am. **285**, 48 (2001).
40) Y. Sugimoto, P. Pou, M. Abe, P. Jelinek, R. Pérez, S. Morita, and Ó. Custance, Nature **446**, 64 (2007).
41) T. Nakamuro, Bull. Chem. Soc. Jpn. **97**, uoae082 (2024).
42) M. Takeguchi, K. Mitsuishi, and A. Hashimoto, Appl. Phys. Express **17**, 085001 (2024).
43) Y. Okawa and M. Aono, Nature **409**, 683 (2001).
44) S. Kawai, O. Krejčí, T. Nishiuchi, K. Sahara, T. Kodama, R. Pawlak, E. Meyer, T. Kubo, and A. S. Foster, Sci. Adv. **6**, eaay8913 (2020).
45) W. Hu, Y. Zhang, and W. Zhou, Appl. Phys. Express **17**, 072003 (2024).
46) N. Oyamada, H. Minamimoto, T. Fukushima, R. Zhou, and K. Murakoshi, Bull. Chem. Soc. Jpn. **97**, uoae007 (2024).
47) H. Mogi, R. Wakabayashi, S. Yoshida, Y. Arashida, A. Taninaka, K. Iwaya, T. Miura, O. Takeuchi, and H. Shigekawa, Appl. Phys. Express **17**, 015003 (2024).
48) K. Hashimoto, K. Amano, N. Nishi, and T. Sakka, Bull. Chem. Soc. Jpn. **98**, uoaf056 (2025).
49) K. Ariga, Nanoscale Horiz. **6**, 364 (2021).
50) T. Tsuchiya, T. Nakayama, and K. Ariga, Appl. Phys. Express **15**, 100101 (2022).
51) N. Shioya, T. Mori, K. Ariga, and T. Hasegawa, Jpn. J. Appl. Phys. **63**, 060102 (2024).
52) K. Ariga, J. Song, and K. Kawakami, Chem. Asian J. **20**, e00836 (2025).
53) K. Ariga, J. Li, J. Fei, Q. Ji, and J. P. Hill, Adv. Mater. **28**, 1251 (2016).
54) J. Song, K. Kawakami, and K. Ariga, Adv. Colloid Interface Sci. **339**, 103420 (2025).
55) G. Chen, T. Koide, J. Nakamura, and K. Ariga, Small Methods **9**, 2500069 (2025).
56) K. Ariga, X. Jia, J. Song, J. P. Hill, D. T. Leong, Y. Jia, and J. Li, Angew. Chem. Int. Ed. **59**, 15424 (2020).
57) R. B. Laughlin and D. Pines, Proc. Natl Acad. Sci. **97**, 28 (2000).
58) K. Ariga, Bull. Chem. Soc. Jpn. **97**, uoad001 (2024).
59) K. Ariga, Materials **18**, 5196 (2025).
60) T. Nakamura, Y. Kondo, N. Ohashi, C. Sakamoto, A. Hasegawa, S. Hu, M. A. Truong, R. Murdey, Y. Kanemitsu, and A. Wakamiya, Bull. Chem. Soc. Jpn. **97**, uoad025 (2024).
61) H. Takane, T. Oshima, T. Harada, K. Kaneko, and K. Tanaka, Appl. Phys. Express **17**, 011008 (2024).
62) K. Saitow, Bull. Chem. Soc. Jpn. **97**, uoad002 (2024).
63) K. Sasaki, Appl. Phys. Express **17**, 090101 (2024).
64) Z. Zhao, Q. Che, Q. Chen, K. Wang, K. Zhao, C. Zhang, H. He, X. Wang, and Y. Chen, Bull. Chem. Soc. Jpn. **97**, uoae083 (2024).
65) M. Shinozaki, T. Johmen, A. Hosaka, T. Seo, S. Yashima, A. Shirachi, K. Noro, S. Sato, T. Kumasaka, and T. Yoshida, Appl. Phys. Express **18**, 075001 (2025).
66) H. Montagu, I. Farrer, D. Ritchie, and S. Kumar, Appl. Phys. Express **18**, 015002 (2025).
67) A. Yamamura, S. Watanabe, M. Uno, M. Mitani, C. Mitsui, J. Tsurumi, N. Isahaya, Y. Kanaoka, T. Okamoto, and J. Takeya, Sci. Adv. **4**, eaao5758 (2018).
68) J. Yu, H. Hanafusa, and S. Higashi, Appl. Phys. Express **17**, 036502 (2024).
69) M. Morimoto, H. Nagahama, and S. Naka, Appl. Phys. Express **17**, 081006 (2024).
70) K. Imaoka et al., Adv. Funct. Mater. **34**, 2409299 (2024).
71) H. Villanti, S. Plissard, J.-B. Doucet, A. Arnoult, B. Reig, L. Dupont, and V. Bardinal, Appl. Phys. Express **18**, 027001 (2023).
72) S. Sarkar, T. Yoshida, B. Prusti, S. R. Jena, K.-C. Ho, and M. Higuchi, ACS Appl. Electron. Mater. **7**, 10651 (2025).
73) K. Ariga, M. Nishikawa, T. Mori, J. Takeya, L. K. Shrestha, , and J. P. Hill, Sci. Technol. Adv. Mater. **20**, 51 (2019).
74) A. Jancik-Prochazkova and K. Ariga, Research **8**, 0624 (2025).
75) H. Bae, H. Ji, K. Konstantinov, R. Sluyter, K. Ariga, Y. H. Kim, and J. H. Kim, Adv. Mater. **37**, e10239 (2025).
76) K. N. Ferreira, T. M. Iverson, K. Maghlaoui, J. Barber, and S. Iwata, Science **303**, 1831 (2004).
77) K. Ariga, Mater. Chem. Front. **1**, 208 (2017).
78) J. Song, A. Jancik-Prochazkova, K. Kawakami, and K. Ariga, Chem. Sci. **15**, 18715 (2024).
79) L. Sutrisno, K. Sun, and K. Ariga, ACS Nano **20**, 6493 (2026).
80) C. Zhang, N. Qian, T. Qin, Q. Chen, J. Liu, H. He, and Y. Chen, Bull. Chem. Soc. Jpn. **97**, uoae119 (2024).
81) H. Tanaka, S. Ito, T. Matsui, and T. Takenobu, Appl. Phys. Express **17**, 031002 (2024).
82) T. Amaya and Y. Otake, Bull. Chem. Soc. Jpn. **98**, uoaf033 (2025).
83) S. Hakata, H. Ishii, H. Takaki, T. Okamoto, J. Takeya, and N. Kobayashi, Appl. Phys. Express **17**, 101001 (2024).
84) T. Mori, Bull. Chem. Soc. Jpn. **98**, uoaf109 (2025).
85) N. Osakabe, A. Yamamura, T. Makita, Y. Tamai, S. Watanabe, and J. Takeya, Appl. Phys. Express **18**, 051001 (2025).
86) K. Maeda, K. Sekizawa, and O. Ishitani, Chem. Commun. **49**, 10127 (2013).
87) P. Giusto, D. Cruz, T. Heil, H. Arazoe, P. Lova, T. Aida, D. Comoretto, M. Patrini, and M. Antonietti, Adv. Mater. **32**, 1908140 (2020).
88) N. Osakabe et al., Sci. Adv. **11**, eadv9952 (2025).
89) T. Okamoto, C. P. Yu, C. Mitsui, M. Yamagishi, H. Ishii, and J. Takeya, J. Am. Chem. Soc. **142**, 9083 (2020).
90) N. Fukui, Bull. Chem. Soc. Jpn. **98**, uoaf062 (2025).
91) H. Kajiwara, M. Mitani, H. Ishii, and T. Okamoto, Appl. Phys. Express **18**, 101002 (2025).
92) G. Kitahara, S. Inoue, T. Higashino, M. Ikawa, T. Hayashi, S. Matsuoka, S. Arai, and T. Hasegawa, Sci. Adv. **6**, eabc8847 (2020).
93) I. Suzuki, J. Hanna, and H. Iino, Appl. Phys. Express **17**, 051007 (2024).
94) S. Yu, W. Deng, X. Wu, Y. Ren, Y. Xie, S. Sun, L. Sun, F. Yang, H.-L. Zhang, and W. Hu, Chem. Soc. Rev. **55**, 567 (2026).
95) B. Fan, G. Liu, Y. Dai, Z. Dong, R. Luan, L. Gong, Z. Zhang, Z. L. Wang, and C. Zhang, Energy Environ. Sci. **17**, 8621 (2024).
96) M. Yamada, Y. Takeda, S. Tokito, and H. Matsui, Appl. Phys. Express **17**, 011010 (2024).
97) J. Liang, H. Zhang, L. Shi, H. Xin, H. Li, and Y. Zhuang, IEEE Sens. J. **25**, 44071 (2025).
98) C. Diacci, J. W. Lee, P. Janson, G. Dufil, G. Méhes, M. Berggren, D. T. Simon, and E. Stavrinidou, Adv. Mater. Technol. **5**, 1900262 (2020).
99) G. Zhou, Z. Cao, Y. Liu, H. Zheng, and K. Xu, J. Electroanal. Chem. **952**, 117961 (2024).
100) C. S. Pundir, V. Narwal, and B. Batra, Biosens. Bioelectron. **86**, 777 (2016).
101) Y.-X. Wang, P.-K. Tsao, M. Rinawati, K.-J. Chen, K.-Y. Chen, C.-Y. Chang, and M.-H. Yeh, Chem. Eng. J. **427**, 131687 (2022).
102) E. V. Karpova, A. I. Laptev, E. A. Andreev, E. E. Karyakina, and A. A. Karyakin, ChemElectroChem **7**, 191 (2020).
103) N. V. Zaryanov, V. N. Nikitina, E. V. Karpova, E. E. Karyakina, and A. A. Karyakin, Anal. Chem. **89**, 11198 (2017).
104) A. M. Pappa, D. Ohayon, A. Giovannitti, I. P. Maria, A. Savva, I. Uguz, J. Rivnay, I. McCulloch, R. M. Owens, and S. Inal, Sci. Adv. **4**, eaat0911 (2018).
105) Y. Shen, S. Chai, Q. Zhang, M. Zhang, X. Mao, L. Wei, F. Zhou, R. Sun, and C. Liu, Chem. Eng. J. **475**, 146008 (2023).
106) Y. Sasaki and T. Minami, Anal. Sci. **41**, 523 (2025).
107) M. Deng, J. Li, B. Xiao, Z. Ren, Z. Li, H. Yu, J. Li, J. Wang, Z. Chen, and X. Wang, Anal. Chem. **94**, 3320 (2022).
108) M. Deng, Z. Ren, H. Zhang, Z. Li, C. Xue, J. Wang, D. Zhang, H. Yang, X. Wang, and J. Li, Adv. Sci. **10**, 2205886 (2023).

109) H. Liu, A. Yang, J. Song, N. Wang, P. Lam, Y. Li, H. K. Law, and F. Yan, Sci. Adv. **7**, eabg8387 (2021).
110) P. Xu, C. Lu, D. Wang, and D. Fu, Microchim. Acta **188**, 301 (2021).
111) Y. Fu, N. Wang, A. Yang, H. K. Law, L. Li, and F. Yan, Adv. Mater. **29**, 1703787 (2017).
112) X. Strakosas et al., Science **379**, 795 (2023).
113) G. Dufil, D. Parker, J. Y. Gerasimov, T.-Q. Nguyen, M. Berggren, and E. Stavrinidou, J. Mater. Chem. B **8**, 4221 (2020).
114) J. Liu et al., Science **367**, 1372 (2020).
115) M. Ito, Y. Yamashita, Y. Tsuneda, T. Mori, J. Takeya, S. Watanabe, and K. Ariga, ACS Appl. Mater. Interfaces **12**, 56522 (2020).
116) M. Ito, Y. Yamashita, T. Mori, M. Chiba, T. Futae, J. Takeya, S. Watanabe, and K. Ariga, Langmuir **38**, 5237 (2022).
117) S. Fujioka, M. Ishii, J. Takeya, K. Ariga, and Y. Yamashita, ACS Appl. Mater. Interfaces **17**, 12488 (2025).
118) C. C. Moser, J. M. Keske, K. Warncke, R. S. Farid, and P. L. Dutton, Nature **355**, 796 (1992).
119) G. Reguera, K. D. McCarthy, T. Mehta, J. S. Nicoll, M. T. Tuominen, and D. R. Lovley, Nature **435**, 1098 (2005).
120) Y. Lin et al., ACS Energy Lett. **5**, 3663 (2025).
121) A. S. Hidayat, N. Ueoka, M. Shimamoto, M. Huda, H. Oshima, Y. Hijikata, A. Muraoka, Y. Nonoguchi, and Y. Matsuo, J. Mater. Chem. A **13**, 42142 (2025).
122) H. Tanaka, K. Kanahashi, N. Takekoshi, H. Mada, H. Ito, Y. Shimoi, H. Ohta, and T. Takenobu, Sci. Adv. **6**, eaay8065 (2020).
123) A. Hawkey, A. Dash, X. Rodríguez-Martínez, Z. Zhao, A. Champ, S. Lindenthal, M. Zharnikov, M. Kemerink, and J. Zaumseil, Adv. Mater. **36**, 2404554 (2024).
124) Y. Kim et al., Adv. Mater. **31**, 1806697 (2019).
125) Y. Liu, B. Nell, K. Ortstein, Z. Wu, Y. Karpov, T. Beryozkina, S. Lenk, A. Kiriy, K. Leo, and S. Reineke, ACS Appl. Mater. Interfaces **11**, 11660 (2019).
126) M. Ishii, Y. Yamashita, S. Watanabe, K. Ariga, and J. Takeya, Nature **622**, 285 (2023).
127) A. Hawkey, X. Rodríguez-Martínez, S. Lindenthal, M. C. F. Jansen, R. Crispin, and J. Zaumseil, Adv. Electron. Mater. **12**, 2400817 (2025).
128) X. Zhan, A. Facchetti, S. Barlow, T. J. Marks, M. A. Ratner, M. R. Wasielewski, and S. R. Marder, Adv. Mater. **23**, 268 (2011).
129) D. M. Leeuw, M. M. J. Simenon, A. R. Browr, and R. E. F. Einerhand, Synth. Met. **87**, 53 (1997).
130) S. K. Mohapatra, S. R. Marder, and S. Barlow, Acc. Chem. Res. **55**, 319 (2022).
131) H. Guo et al., Nature **599**, 67 (2021).
132) Y. Yamashita, S. Kohno, E. Longhi, S. Jhulki, S. Kumagai, S. Barlow, S. Marder, J. Takeya, and S. Watanabe, Commun. Mater. **5**, 79 (2024).
133) M. Xiong et al., Nat. Commun. **15**, 4972 (2024).
134) T. Ohashi, M. Ishii, J. Takeya, K. Ariga, and Y. Yamashita, Small **21**, e09278 (2025).
135) K. Akaike, T. Hosokai, Y. Ono, R. Tsuruta, and Y. Yamada, Adv. Mater. Interfaces **10**, 2201800 (2023).
136) L. Yuan et al., Nat. Mater. **23**, 1268 (2024).
137) Z. Xiao, M. Ishii, J. Takeya, K. Ariga, and Y. Yamashita, J. Mater. Chem. C **12**, 12739 (2024).
138) H. Sun, M. Ishii, J. Takeya, K. Ariga, and Y. Yamashita, npj Soft Matter **2**, 2 (2026).

Takuma Ohashi was born in 2000. Graduated from the Department of Pure and Applied Chemistry, Faculty of Science and Technology, Tokyo University of Science in 2023. Completed the Master's program in Department of Pure and Applied Chemistry at the Graduate School of Science and Technology, Tokyo University of Science, in 2025. Currently pursuing a Ph.D. at the same graduate school, conducting research on doping methods for n-type organic semiconductors.

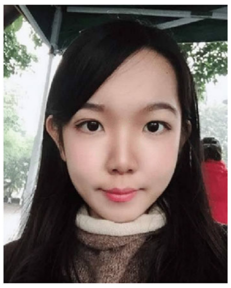

Linawati Sutrisno received her Ph.D. degree in 2022 from University of Tsukuba. She began her research career as a postdoctoral researcher at the National Institute for Materials Science (NIMS) in 2022. After her postdoctoral work at NIMS, she continued her research as a JSPS Research Fellow and currently works as an independent research fellow at International Center for Young Scientists (ICYS). Her research interests include in vitro imaging technologies aimed at developing strategies for cancer treatment and tissue regeneration, as well as the development of 3D porous scaffolds for bone, adipose, and skin tissue regeneration.

Yu Yamashita received his Ph.D. in Science from the University of Tokyo in 2019. He is currently a senior researcher at the National Institute for Materials Science (NIMS), Japan, and an associate professor at the University of Tokyo. His research focuses on chemical doping of molecular semiconductors, carrier transport mechanisms, and structure–property relationships in organic molecular thin films, as well as their applications in electronic devices such as diodes, transistors, and electrochemical transistors.

Katsuhiko Ariga received his Ph.D. from the Tokyo Institute of Technology in 1990. Following research positions at Tokyo Institute of Technology, University of Texas at Austin, JST Supermolecule Project, Nara Institute of Science and Technology, and JST Nanospace Project, he joined National Institute for Materials Science (NIMS) in 2004. He is currently the leader of the Supermolecule Group and a senior scientist with special missions at Research Center for Materials Nanoarchitectonics (MANA) at NIMS. He is also a professor at University of Tokyo. His primary research interests lie in exciting and innovative topics in supramolecular chemistry, interfacial science, thin film technology, and nanoarchitectonics.